

The revised GB/GB2 sample of extragalactic radio sources^{*}

J. Machalski¹

Obserwatorium Astronomiczne, Uniwersytet Jagielloński, ul. Orła 171, 30-244 Kraków, Poland

Received April 16; accepted June 25, 1997

Abstract. This paper presents the revised sample of 373 extragalactic radio sources brighter than 0.2 Jy at 1.4 GHz. These sources, selected from the finding Green Bank surveys, were mapped at 1465 MHz using the VLA at different configurations. The biases introduced into the original GB and GB2 catalogues by confusion as well as partial resolution by the VLA at A-configuration, are eliminated. In effect, a number of sources have been excluded, and a few other are included into the revised sample. Now the sample is about 99, 97, and 95 per cent complete for sources with $S_{1.4} \geq 0.55$ Jy, $0.25 \text{ Jy} \leq S_{1.4} < 0.55$ Jy, and $0.2 \text{ Jy} \leq S_{1.4} < 0.25$ Jy, respectively. A compilation of the radio, optical, and X-ray data available for the sample sources are presented in Table 3. New 4.9-GHz VLA images of selected sources are included. A number of statistics describing radio morphological and spectral contents of the sample, radio variability, revised source counts, redshift distributions, etc. are given.

Key words: surveys — quasars: general — galaxies: active — radio continuum: general; galaxies

1. Introduction

Statistically complete samples of extragalactic radio sources, providing as much as possible information about their physical and geometrical parameters, radio structure and morphology, optical and X-ray counterparts, etc., are still of great importance for further astrophysical and cosmological studies. The best studied samples, complete within a defined sky area and flux-limited only, were selected from finding surveys of the sky carried out at a num-

ber of frequencies. In particular, much observational attention have been given to the brightest sources at 178 MHz (10-Jy sample: Laing et al. 1983, and references therein), 408 MHz (B3-VLA sample: Vigotti et al. 1989), 2.7 GHz (2-Jy sample: Wall & Peacock 1985; cf. also Morganti et al. 1993; Tadhunter et al. 1993), and 5 GHz (S5 sample: Kühn et al. 1981; 1.3-Jy sample: Pearson & Readhead 1988; CJ1 0.7-Jy sample: Polatidis et al. 1995).

A similar effort has been undertaken at 1.4 GHz. About 240 intermediate-strength radio sources stronger than 0.55 Jy and located within a sky area of 0.44 sr were selected by Machalski & Maslowski (1982) (hereafter referred to as Paper I) from the GB and GB2 finding surveys, and afterwards supplemented with those having $S \geq 0.2$ Jy and $S \geq 0.25$ Jy, respectively, in two smaller regions corresponding the area of 0.09 sr (Machalski & Condon 1983b). The sample sources were then observed with the VLA at 1465 MHz or 1490 MHz in its partial (P) or A-configuration. High-resolution (1.3 – 2.5 arcsec) maps were provided for all the sources (Machalski et al. 1982; Paper II, Machalski & Condon 1983a,b; Papers III and IV, respectively). Strongly resolved and/or confused sources were reobserved with the VLA C-array, providing low-resolution maps (Machalski & Condon 1985a; Paper V). As a result, the radio structure, angular size, asymmetry, bending, etc. could be determined for the extended sources. As expected, the sample consists of a large fraction of compact sources, unresolved with the VLA synthesized beam of about 1.2 – 1.3 arcsec; those were analysed by Machalski & Inoue (1990).

The described VLA observations showed that several GB and GB2 radio sources were strongly confused by a fainter companion closer than about 6 – 7 arcmin, or even appeared to be a cluster of a few nearby sources unresolved with the $\approx 10 - 11$ arcmin beam of the NRAO 91 m telescope used in the finding surveys. Furthermore, the information content of the sample concerning optical identification, photometry, redshift, X-ray counterpart, etc., has grown since the above publications due to our own observational efforts, as well as results published by other

Send offprint requests to: J. Machalski
e-mail: machalsk@oa.uj.edu.pl

* Table 3 and notes to Table 3 are also available in electronic form at CDS via anonymous ftp to cdsarc.u-strasbg.fr (130.79.128.5) or via <http://cdsweb.u-strasbg.fr/Abstract.html>

authors investigating objects common with the GB/GB2 sample.

The present paper concludes the sample revising its completeness to the limiting flux of 0.2 Jy, and providing a compendium of the radio, optical, and X-ray parameters for the sample sources. In Sect. 2 a definition of the sample is given, and its completeness is estimated. Designation of the radio spectrum, morphology, and variability is given in Sect. 3, while the optical identification with galaxies and quasars, their magnitudes and redshift, are verified in Sect. 4. The radio, optical, and recent X-ray data for the sample sources are summarized in Sect. 5. Some statistical results: radio morphology and optical identification contents of the sample, revised 1.4-GHz source counts around their peak at about 0.6 Jy, precise spectral-index distributions, and redshift distributions, are described in Sect. 6.

2. The sample

2.1. Definition of the sample

The sample is defined as follows:

Part 1: 233 sources with $S_{1.4} \geq 0.55$ Jy (hereafter on the Baars et al. 1977 scale) within the B(1950) sky coordinates: $7^{\text{h}}17^{\text{m}} < \alpha < 16^{\text{h}}23^{\text{m}}$, $+45^{\circ}8 < \delta < +51^{\circ}7$ and $7^{\text{h}}08^{\text{m}} < \alpha < 16^{\text{h}}58^{\text{m}}$, $+31^{\circ}8 < \delta < +39^{\circ}7$. Sky area of 0.4414 sr.

Part 2: 109 sources with $0.25 \text{ Jy} \leq S_{1.4} < 0.55 \text{ Jy}$ within $7^{\text{h}}15^{\text{m}} < \alpha < 13^{\text{h}}11^{\text{m}}$, $+48^{\circ}0 < \delta < +50^{\circ}0$, $7^{\text{h}}08^{\text{m}} < \alpha < 9^{\text{h}}08^{\text{m}}$, $+34^{\circ}5 < \delta < +38^{\circ}0$, and $9^{\text{h}}08^{\text{m}} \leq \alpha < 16^{\text{h}}57^{\text{m}}$, $+34^{\circ}5 < \delta < +35^{\circ}5$. Sky area of 0.0906 sr.

Part 3: 31 sources with $0.20 \text{ Jy} \leq S_{1.4} < 0.25 \text{ Jy}$ within $7^{\text{h}}08^{\text{m}} < \alpha < 9^{\text{h}}08^{\text{m}}$, $+34^{\circ}5 < \delta < +38^{\circ}0$, and $9^{\text{h}}08^{\text{m}} \leq \alpha < 16^{\text{h}}57^{\text{m}}$, $+34^{\circ}5 < \delta < +35^{\circ}5$. Sky area of 0.0550 sr.

All the sources have $b_{\text{II}} > 20^{\circ}$. Hereafter these parts are referred to as Subsample 1, 2, and 3, respectively.

2.2. Mean weighted 1.4-GHz flux density

For all the sample sources their two independent measurements of 1.4 GHz flux density resulting from the Green Bank surveys GB/GB2 (Maslowski 1972; Machalski 1978a) and 83GB (Condon & Broderick 1985; the relevant catalogue by White & Becker 1992) were compared with the measured VLA flux density (cf. Introduction). That comparison allowed to select either confused sources requiring flux correction or heavily resolved sources for further reobservations with lower resolution. Some of the confused sources appeared to be two different ones but still satisfying the criteria of the sample. Recently D-array and B-array maps for several of the sample sources have become available from the large VLA 1.4-GHz sky surveys: FIRST by Becker et al. (1995) and Condon et al. (1996). These were also used to check the effects of resolution in our data.

For many of the sources, additional 1.4 GHz fluxes were also available from observations with the Effelsberg 100 m telescope (Kühr et al. 1981) and Arecibo 300 m telescope (Owen et al. 1983); some fluxes for compact sources were available from measurements with the WSRT and Cambridge One-mile (OMT) telescopes. All collected 1.4 GHz flux densities, corrected for confusion if necessary, were then used to compute the weighted mean flux density at this frequency, $\langle S_{1.4} \rangle$, and its error, σ , with the standard formulae

$$\sigma^2 = \left[\sum_i (1/\sigma_i^2) \right]^{-1} \quad \langle S_{1.4} \rangle = \sum_i (S_i \sigma_i^2 / \sigma_i^2). \quad (1)$$

The mean 1.4-GHz flux density was used to verify completeness of the sample.

2.3. Completeness of the sample

In order to satisfy the conditions given in Sect. 2.1, 12 sources from Paper I and 20 sources observed in Papers IV and V have been excluded from the sample. They are listed in Table 1 with information about the cause of exclusion. In turn, 15 sources have been added to the sample because they were underestimated in the finding surveys due to a large flux density error but their mean 1.4-GHz flux density calculated from all available observations (cf. Sect. 2.2) satisfied the selection criterion. These additional sources are indicated by a diamond mark (\diamond) preceding the source name in Table 3. Due to the above corrections, we estimate that now the sample is about 99 per cent complete for sources with $S_{1.4} \geq 0.55$ Jy, about 97 per cent complete for sources with $0.25 \text{ Jy} \leq S_{1.4} < 0.55 \text{ Jy}$, and about 95 per cent complete for sources with $0.20 \text{ Jy} \leq S_{1.4} < 0.25 \text{ Jy}$. The completeness is evaluated using the method of Dixon & Kraus (1968).

3. The radio data

3.1. Radio spectrum and spectral index

In order to determine the radio spectrum for each source of the sample, we relied on a number of radio source catalogues, especially on: 151-MHz 6CII, III, and IV (Hales et al. 1993; and references therein, 365-MHz Texas (Douglas et al. 1980), 408-MHz B2 and B3 (Colla et al. 1973 and Ficarra et al. 1985, respectively), 1.4-GHz Arecibo observations in the sky strip $+34^{\circ}5 < \delta < +35^{\circ}5$ (Owen et al. 1983) and 83GB (White & Becker 1992), 4.8-GHz GB6 (Gregory et al. 1996) and MGII and MGIV (Langston et al. 1990 and Griffith et al. 1991, respectively). The flux densities were adjusted to the common scale of Baars et al. (1977). Errors of the flux density were taken directly from the individual papers or calculated according to the formulae given there. A fitting the data points with a polynomial function of the type

Table 1. (*left panel*): Sources excluded from the Part 1 (list of Machalski & Maslowski 1982); (*central and right panel*): excluded from the Part 2 and Part 3 (lists of Machalski & Condon 1983b, 1985)

Source	Cause	Source	Cause	Source	Cause	Note
0724+467	$S < 0.55$ Jy	0719+362	2 sources	1137+493	$S < 0.25$ Jy	
0738+336	2 sources	0728+364	2 sources	1202+488	cluster	
0908+340	2 sources	0846+377	2 sources	1204+483	2 sources	
0913+471	$S < 0.55$ Jy	0851+363	2 sources	1205+500	2 sources	
0914+502	$S < 0.55$ Jy	0902+480	2 sources	1225+498	2 sources	
1112+333	2 sources	0910+486	$S < 0.25$ Jy	1316+346	$S < 0.20$ Jy	
1135+464	2 sources	0954+490	2 sources	1401+350	cluster	a)
1317+362	2 sources	0955+492	3 sources	1533+345	cluster	
1432+382	3 sources	1042+481	$S < 0.25$ Jy	1539+350	$S < 0.20$ Jy	
1442+363	2 sources	1124+488	cluster	1648+350	2 sources	
1614+473	$S < 0.55$ Jy					
1615+352	part of 1615+351?					

a) given in Machalski & Condon (1990).

$y = a + bx + cx^2 + d \cdot \exp(\pm x)$, where $y = \log S$, $x = \log \nu$, was performed.

Three cases are considered: (1) a straight line, where $c = d = 0$ (s-spectrum), (2) a curved fit, where $c = 0$ or $d = 0$ (c- or c+ spectrum), and (3) a composite fit, where $b, c, d \neq 0$ (+c- spectrum if $b > 0$ and $d < 0$, or -c+ spectrum if $b < 0$ and $d > 0$). The reduced χ^2 -test was used to decide whether the data could be fitted with either of the above functions. The spectra which could not be adequately fitted to the data (typical for variable sources) are considered to be complex (cpx-spectrum). In some sources the best fitted spectrum consists of two straight lines with a break frequency (sb-spectrum).

The fitted spectrum was then used to determine a spectral index as a derivative (i.e. a slope) of the above type function at the frequency of 1.4 GHz, $\alpha_{1.4}$. Thus, using a functional form of the spectrum, one has two advantages in respect to the popular two-point spectral indices: (i) the slope is not affected by the errors of individual flux density measurements, and (ii) it can be easily transformed into another frequency, e.g. emitted one. In Sect. 6, statistics of the spectra and distributions of $\alpha_{1.4}$ are given and discussed.

3.2. Radio morphology

The radio morphology is determined mostly on the basis of VLA maps published in Papers II, III, IV, and V. Because the strongest sample sources (mostly 3C sources with $S_{1.4} > 2$ Jy), as well as strong compact sources which had been already observed with the VLA by Perley (1982), were not reobserved during the GB/GB2 project, their morphology was specified from other publications. Extended double sources are classified either as edge-brightened (FRII) or edge-darkened (FRI)(classification of Fanaroff & Riley 1974), although morphological type of

some of the sources should be determined as an intermediate type.

The other sources have either compact structure dominated by a flat-spectrum unresolved radio core, frequently with weak one-sided (C + 1s) or two-sided (C + 2s) extended emission detected with the VLA, or compact steep-spectrum (CSS) structure. In some cases a distinction between these two types is not easy. A compact source with well fitted spectrum of “s” or “c-” type is classified as CSS regardless of a frequency of the maximum of its fitted spectrum, while a compact core-dominated source with detected or undetected “1s” or “2s” emission, having more complex spectrum of “cpx”, “+c-” or “-c+” type is considered here as a separate morphological category. It was shown by Machalski & Inoue (1990) that the GB/GB2 sources with deconvolved angular size $\theta < 1 - 1.5$ arcsec differ significantly in the fringe visibility function, suggesting a variety of structures on the angular scale of about 0.1 – 0.5 arcsec, and have radio spectra which can be only conventionally classified as flat or steep. The distribution of $\alpha_{1.4}$ for the CSS sources (Fig. 1) illustrate the problem.

The morphological types and structural parameters of the sources added to the sample have been taken from available maps of the NVSS and FIRST surveys, or from our own, unpublished, VLA maps. The observed structures were crudely deconvolved into elliptical Gaussian components; relevant data, i.e. their map coordinates, integrated 1.4 GHz flux density, half-intensity major and minor diameters, major-axis position angle (degrees east of north), as well as the source’s “largest angular size” *LAS* and “overall position angle” *OPA*, are given in the Appendix (Table A1).

3.3. 1.4-GHz radio variability

Due to the large time base of the 1.4-GHz observations (Sect. 2.2), from 8 to 13 years, and a sufficient number of independent flux measurements, it was possible to determine the sample sources which vary significantly at this frequency. The 1.4-GHz variability in the GB/GB2 sample was the subject of separate analyses (Ryś & Machalski 1990; Machalski & Magdziarz 1993a). After supplementing older data in the sample with those already available from the NVSS and FIRST surveys, the time base over which the 1.4-GHz variability has been observed extends to 18–24 years. Compactness of these sources and the lack of nearby confusing neighbours (except of 0804+499B, whose flux densities have been carefully corrected for confusion) provide that their flux densities measured with single-dish telescopes and the VLA are comparable.

The variable sources in the sample are listed in Table 2. For each source, the variability parameters as defined by Machalski & Magdziarz (1993a), i.e. the number of independent observations, n , mean weighted 1.4-GHz flux density and its error (calculated with Eqs. (1)), chi-squared statistics, “apparent fluctuation” of flux density around its mean value, $Y(n)$ (the $Y(n)$ statistics has the physical meaning of the quantity $(S_{\max} - S_{\min}) / (S_{\max} + S_{\min})$, but is not numerically identical with it), and time lag between the first and last observations, T , are given in consecutive columns of Table 2. Note that all of these variables but one (1213+350) are of complex (cpx) spectrum with $\alpha_{1.4} < 0.5$. It is worth to emphasize that most of these sources are known to be variable at frequencies higher than 1.4 GHz; those which were or are systematically monitored for variability are marked in the last column of Table 2.

4. The optical and X-ray data

4.1. Optical identifications

The radio sources were identified with their optical counterpart on the basis of its positional coincidence with the radio centre. If a compact radio core was detected, then it undoubtedly coincided with the identification. If a source was an extended one and no core could be detected, then a much larger area near the “centre” of the source had to be considered. Usually the source was identified with the brightest galaxy or stellar object in the “centre”. Majority of the sample sources were identified with galaxies and quasars, as well as galaxy or quasar candidates seen on the Palomar Observatory Sky Survey (POSS) prints. The tentative samples of GB/GB2 radio galaxies and quasar candidates were analyzed by Machalski & Condon (1985b, 1986). Later on, deeper identifications were collected from the literature and our own research (e.g. Machalski & Magdziarz 1993b). In Notes to Table 3 some ambiguous identifications are discussed. Unfortunately, still about 34

Table 2. The sample sources variable at 1.4 GHz

Source	n	$\langle S_{1.4} \rangle$ [mJy]	σ [mJy]	χ^2	$Y(n)$	T [yr]	Note
0711+356	7	1642	12	190.0	0.08	24.1	
0723+488	4	473	5	87.0	0.10	24.0	
0748+333	5	684	6	191.6	0.11	19.2	
0804+499B	5	846	11	180.2	0.16	24.0	a)
0828+493	6	1123	10	466.0	0.18	23.8	a)
0923+392	9	2666	32	79.7	0.07	24.2	a)b)c)
1015+359	5	653	11	71.6	0.13	24.1	a)
1128+385	5	756	8	49.1	0.07	18.3	a)
1144+352	6	555	9	93.2	0.13	18.3	
1155+486	3	330	15	46.9	0.37	13.0	
1213+350	6	1522	20	34.6	0.06	18.6	a)
1239+376	4	569	12	44.8	0.14	19.2	
1308+326	6	1405	17	255.6	0.15	18.8	b)c)
1600+335	6	2660	19	32.5	0.03	23.8	
1611+343	7	2854	17	391.8	0.09	23.8	b)
1633+382	7	2112	15	639.8	0.13	23.8	a)b)c)
1656+348	8	454	6	60.3	0.08	18.4	a)

a) variable at 10.8 GHz (Seielstad et al. 1983)

b) monitored at 4.8, 8.0, and 14.5 GHz (Hughes et al. 1992)

c) monitored at 22.2 and 36.7 GHz (Valtaoja et al. 1992).

per cent of the sources in Part 1, about 45 per cent in Part 2, and about 52 per cent in Part 3 remain unidentified.

4.2. Optical magnitudes and redshift

Red (R) and blue (B) magnitudes of the identified objects are either photometric ones in the R Kron–Cousins VRI system (Cousins 1976) and in the UBV system of Johnson (1966), or estimated from the POSS(E) and POSS(O) prints, respectively. In particular, $UBVRI$ photometry for the brightest elliptical galaxies and quasars in the sample was provided by Machalski & Wiśniewski (1988), and absolute M_R and M_B magnitudes as well as four intrinsic colours of the elliptical galaxies, corrected for galactic extinction, aperture, and reddening (K-correction), was given by Machalski (1988). Statistics of the optical type is given in Sect. 6.

Spectroscopic redshift is available for majority of the sample quasars, and for many brighter galaxies. References to the available photometry and redshifts are provided in Table 3. For elliptical galaxies without spectroscopic redshift but with photoelectrical photometry, a redshift estimate, based on corrected R -magnitude and $B-R$ colour, is provided by Machalski (1988). A statistical analysis, described in Sect. 6 suggests that at least 11–12 sources in the sample may have redshift greater than 3.16.

4.3. X-ray identifications

The sample sources are identified with X-ray sources observed with the Imaging Proportional Counter (IPC) on the EINSTEIN observatory (Wilkes et al. 1994), and the Position Sensitive Proportional Counter (PSPC) on the ROSAT observatory. The latter data were taken from the “WGA” catalogue, and an updated version of the “First ROSAT source Catalogue of Pointed Observations”. An X-ray source is considered as a counterpart for a radio source if its normalized distance to the radio position is

$$d = [(\Delta\alpha/\sigma_\alpha)^2 + (\Delta\delta/\sigma_\delta)^2]^{1/2} < 2.5 \quad (2)$$

where: $\Delta\alpha$ and $\Delta\delta$ are the differences between the X-ray and radio position, and σ_α and σ_δ are the combined X-ray–radio position errors $\sigma_i = (\sigma_{X\text{-ray}}^2 + \sigma_{\text{rad}}^2)^{1/2}$ in right ascension and declination, respectively. Majority of the X-ray sources are identified with compact radio sources (mostly quasars and BL Lac objects) for which accuracy of the VLA position is $\sigma_{\text{rad}} \approx 0.1 - 0.2$ arcsec.

Because the X-ray data available are not homogeneous, and the GB/GB2 sky region is only partly covered by the above X-ray observations, their details (epoch of observation, integration time, resultant counts, etc.) are not cited in this paper. Only a reference to the original data is given.

5. Summary of the radio, optical, and X-ray data

Radio, optical, and X-ray data for the sources in the revised GB/GB2 sample are summarized in Table 3, whose format is as follows:

Column 1: IAU-format source name.

Column 2: Sequence of 10 consecutive marks indicating whether the source appears in the following catalogues: (1) 151 MHz: 6CII, III, VI (Hales et al. 1993; and references therein), (2) 178 MHz: 4C (Pilkington & Scott 1965; Gower et al. 1967), (3) 365 MHz: Texas (Douglas et al. 1980), (4) 408 MHz: B2 (Colla et al. 1972; 1973), (5) B3 (Ficarra et al. 1985), (6) 750 and 1400 MHz: NRAO (Pauliny-Toth et al. 1966), (7) 966 MHz: Jodrell Bank (Cohen et al. 1977; Porcas et al. 1980), (8) 1400 MHz: 83GB (Condon & Broderick 1985; White & Becker 1992), (9) 4830 MHz: MGII (Langston et al. 1990); MGIV (Griffith et al. 1991), (10) 4850 MHz: GB6 (Gregory et al. 1996). “*”–presence; “/”–absence; “c”–flux contaminated by confusing source or sources; “r”–source resolved, flux underestimated.

Column 3: “1”, “2”, and “3” denotes that the source belongs to Subsample 1, 2, and 3, respectively. “1, 2” denotes sources with $S \geq 0.25$ Jy in the area of 0.0906 sr, and “2, 3” denotes sources with $0.20 \text{ Jy} \leq S < 0.55 \text{ Jy}$ in the area of 0.0550 sr.

Column 4: Weighted mean 1.4-GHz flux density and its rms error (in mJy). “v” denotes the standard deviation of variable flux (given in parentheses) instead of error of the mean.

Column 5: Slope of the fitted spectrum at 1.4 GHz and its rms error. The slope is the derivative of a function $y = a+bx+cx^2$ or $y = a+bx+d \cdot \exp(\pm x)$ (cf. Sect. 3.1). If no function could be fitted to the spectral data (generally for variable sources), a crude slope at 1.4 GHz is given in parentheses.

Column 6: Type of radio spectrum (cf. Sect. 3.1).

Column 7: Radio morphology (cf. Sect. 3.2). FRI–edge-darkened double, FRII–edge-brightened double (Fanaroff & Riley 1974); C–compact, unresolved; C(1s), C(2s)–core-dominated compact with one-sided or two-sided extended emission, respectively. “cc” appended to the type denotes that a compact core has been detected, “CSS”–compact steep-spectrum, “Di”–diffuse emission.

Column 8: Largest angular size in arcsec.

Column 9: Code concerning the VLA maps available. “1.4” and sometimes “4.9” indicate observing frequency, and upper-case letters — VLA configuration used for observations (“P” means partially completed VLA in 1980). An asterisk (*) denotes that no map is available, and the source is represented by fitted Gaussian components only. If a VLBI-scale structure has been observed in the compact source, this is indicated.

Column 10: Source name repeated.

Column 11: Optical type. GAL — galaxy confirmed spectroscopically and/or with an extended image; (GAL) — possibly a galaxy; GAL? — identification ambiguous; QSO — quasar confirmed spectroscopically; BL — BL Lac object; RSO, NSO, BSO — red, neutral, and blue stellar object, respectively (most of NSOs and BSOs are quasar candidates); RO, BO — red, and blue object too faint to be recognized as stellar or extended. EF — “empty field” source, an identification likely beyond the POSS limit. “X” preceding the type indicates that an X-ray source coincides with the radio position.

Column 12: Redshift. A value in parentheses has been estimated from the apparent magnitude and colour (cf. Sect. 4.2).

Columns 13 and 14: *R*– and *B*–magnitudes. Two decimal digits precision indicate magnitudes measured with photoelectric or CCD photometry.

Columns 15 and 16: J(2000) sky coordinates. “o” preceding right ascension denotes the optical object’s position. For double source without a radio core, the given position corresponds to a radio centroid.

Column 17: References to the large-scale radio structure and VLA maps, VLBI-scale structure, photometry, and redshift.

Column 18: “+” marks that a note to the source is appended.

Table 3. The revised GB/GB2 sample (The table is attached separately).

6. The statistics

6.1. Spectral content

The spectral index at 1.4 GHz, $\alpha_{1.4}$, besides the total flux density at this frequency, is one of the best determined parameters of the GB/GB2 sources.

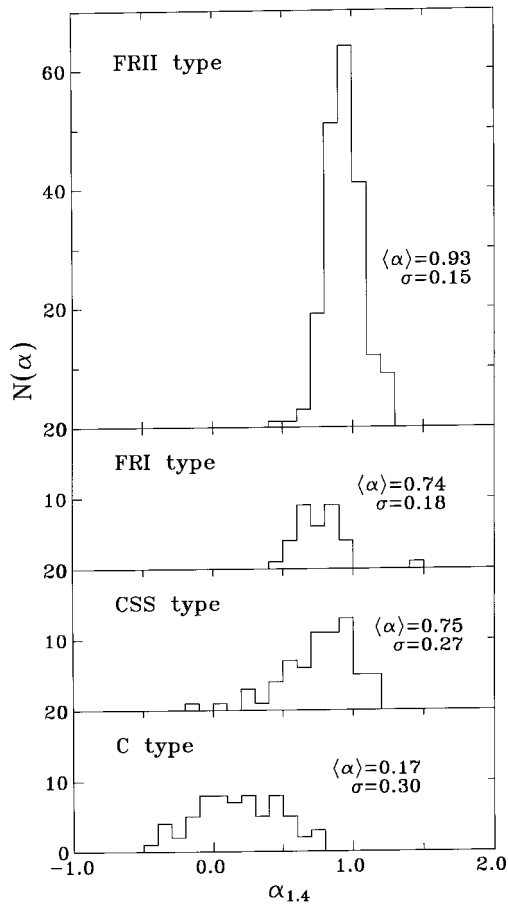


Fig. 1. Spectral-index $\alpha_{1.4}$ distributions of sources of different morphological type. $\alpha_{1.4}$ is a slope of the fitted spectrum at 1.4 GHz (cf. Sect. 3.1). Their mean values and standard deviations are indicated

The distribution of $\alpha_{1.4}$, for four different morphological types is shown in Fig. 1. The distribution of $\alpha_{1.4}$ for different optical classes: galaxies, QSOs, and undetected (EF) sources, is shown in Fig. 2.

The mean values and standard deviations of these distributions are given on the relevant histograms. The standard deviations of $\alpha_{1.4}$ are always smaller than the corresponding deviation of any two-point spectral index.

The distributions of $\alpha_{1.4}$ obtained for the FRII and FRI as well as C sources are highly symmetrical. Momental skewness of the $\alpha_{1.4}$ distributions of FRII and FRI sources taken altogether is 0.036; the same of the

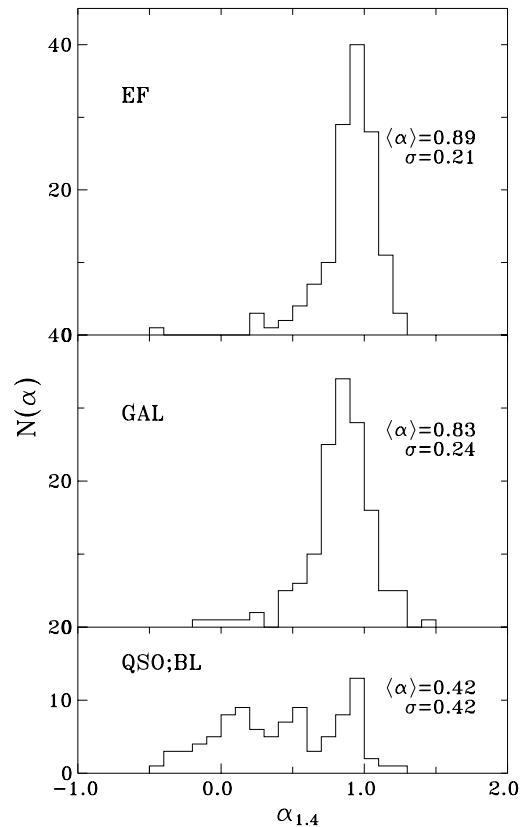


Fig. 2. The same as in Fig. 1 but for sources of different optical type

C sources is only 0.007. In turn, the large skewness of 1.089 for the CSS sources is evidently caused by different morphological types (small projected doubles, very compact self-absorbed sources, steep-spectrum core-jet structures, and complex sources which do not fit into any of the above categories) constituting the entire CSS class (e.g. Sanghera et al. 1995). The highly symmetrical spectral-index distributions of the lobe-dominated and core-dominated sources support the assumption about a Gaussian functional form which were frequently used to describe these distributions in cosmological evolutionary models (cf. Petrosian & Dickey 1973; Kulkarni 1978; Condon 1984).

6.2. Optical identification content

For some GB/GB2 sources the optical type is uncertain. This is the case with the faintest objects barely visible on the POSS prints or detected by the CCD imaging beyond the POSS limit. Nevertheless for the statistical purpose, taking also into account their radio morphology and spectrum, one can include them into one of the two main categories: galaxy or quasar. Such a simplified optical identification content of the sample is given in Table 4. For each

flux density range, the first row gives the fractions of all available identifications; the second - the corresponding fractions if optical identification is limited to $R < 20$ mag (the POSS limit).

Table 4. The optical type vs. flux density range, cf. the text

$\Delta S(\text{Jy})$	Galaxy	QSO	EF	sum
> 2.0	15(63% \pm 10%)	7(29% \pm 9%)	2(8% \pm 6%)	24
	11(46% \pm 10%)	6(25% \pm 9%)	7(29% \pm 9%)	
0.55–2.0	84(40% \pm 4%)	54(26% \pm 3%)	71(34% \pm 4%)	209
	62(30% \pm 4%)	45(22% \pm 3%)	102(49% \pm 7%)	
0.25–0.55	33(30% \pm 5%)	27(25% \pm 4%)	49(45% \pm 5%)	109
	15(14% \pm 4%)	21(19% \pm 4%)	73(67% \pm 5%)	
0.20–0.25	8(26% \pm 8%)	7(23% \pm 8%)	16(52% \pm 9%)	31
	5(16% \pm 7%)	6(19% \pm 8%)	20(65% \pm 10%)	

The fraction of QSO identifications is similar in the different flux-limited subsamples; a decrease of the fraction with flux density is statistically insignificant. Limiting the optical identification to $R < 20$ mag, this fraction decreases by about 4 per cent only in each flux range. The above is consistent with the independence of the radio properties of radio-loud quasars on their optical luminosities (e.g. Peacock et al. 1986). Some enlargement of the

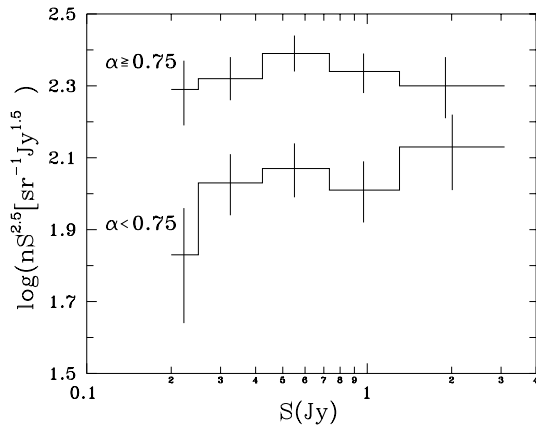


Fig. 3. Normalized differential counts of “steep-spectrum” and “flat-spectrum” GB/GB2 sources at 1.4 GHz

QSO fraction is expected after further identifications of the EF sources. Basing on the optical luminosity function of quasars and their radio-to-optical luminosity ratio function (cf. Machalski 1996), about 25 ± 5 more QSOs with $R \geq 20$ mag and $S_{1.4} > 200$ mJy can be expected. Furthermore, a decrease of the galaxy identifications with decreasing flux density limit is evident. Therefore, most

of the EF sources should be distant powerful galaxies. A distribution of the optical type for different radio morphologies is shown in Table 5.

Table 5. The optical type vs. radio morphology

Morph.	Galaxy	QSO	EF	sum
FRII	85(42% \pm 5%)	26(13% \pm 2%)	92(45% \pm 4%)	203
FRI	29(85% \pm 6%)	2(6% \pm 4%)	3(9% \pm 5%)	34
CSS	19(28% \pm 6%)	11(16% \pm 5%)	38(56% \pm 6%)	68
C	5(8% \pm 3%)	56(84% \pm 5%)	5(8% \pm 3%)	66
Disk	2			2

A majority of FRI type emission is connected to radio galaxies, while most of C types, frequently with one-sided (1s) or two-sided (2s) emission detected besides the bright core, are related to QSOs. However, there is no clear distinction between FRI and large C+2s radio sources. Usually a linear extent of C+1s or C+2s structure does not exceed the size of a parent optical object, i.e. about 10–15 kpc. However, in some quasars two-sided emission extends over much larger distances from the core; these are classified here as FRI (e.g. 0827+378, 1148+387). Concerning the FRII sources, we estimate that no more than 10 per cent of EF sources in the sample can be quasars; the remaining ones should be distant galaxies. The compact steep-spectrum (CSS) sources are found both in galaxies and QSOs. The relatively large fraction of CSS EF sources suggests that they are very distant.

6.3. Source counts

6.3.1. The spectrum-dependent counts

The counts of all radio sources at 1.4 GHz are very well established down to a sub-mJy level (e.g. Windhorst et al. 1985). The first limited spectral counts at this frequency were published by Machalski (1978b), but over almost two decades had remained unimproved, and were not used, for example, to constrain the cosmological models. However, such constraints at 2.7 and 5 GHz were successfully applied to the evolutionary models of Condon (1984) and Dunlop & Peacock (1990).

Although dividing of sources into “flat-spectrum” and “steep-spectrum” populations, in the face of “unified models”, is now by large unjustified; spectrum-dependent counts can be still useful for cosmological purposes. For these purposes, the source population can be separated into two subpopulations with an arbitrarily chosen spectral index. Such differential counts of the sample sources with $\alpha_{1.4} < 0.75$ and $\alpha_{1.4} \geq 0.75$, normalized to the Euclidean ones, are shown in Fig. 3. Numerical data of these counts, extended to a lower flux density limit on the basis of other 1.4-GHz samples, will be published in

a forthcoming paper (Machalski & Jamrozy, in preparation).

6.3.2. The radio type-dependent counts

There are already indications that the spatial distributions of sources of different morphological type are not identical, i.e. these sources could evolve differently in cosmic time. While there is no doubt that the powerful radio galaxies and quasars show a strong evolution; the amount of evolution of low-power sources (mJy-level radio galaxies, Seyferts, etc.) is still controversial. Even among powerful

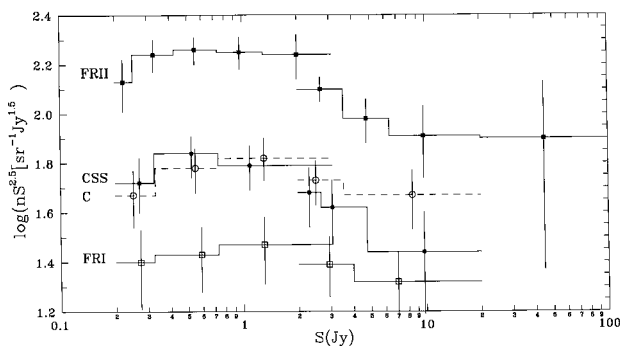


Fig. 4. Normalised differential counts of sources of different morphological type at 1.4 GHz

sources the amount of cosmological evolution may not be the same for separate types (e.g. FRI and FRII).

In order to enable the use of the GB/GB2 data for exploring the implications of unified-model schemes, the normalised differential counts of the FRII, FRI, CSS, and C sources are provided in Fig. 4.

After extending these counts to the flux density of 100 Jy (taking into account the sources with $2 \text{ Jy} < S_{1.4} < 100 \text{ Jy}$ in the sky area of 4.22 sr ; $\delta > 10^\circ$, $|b_{\text{II}}| \geq 10^\circ$) it can be seen that the counts of FRI sources to the flux limit of 0.2 Jy are much flatter than the corresponding counts of FRII sources. Also the counts of the CSS and C sources probably differ between themselves, although the statistics available here is not sufficient to prove this. A further study of the above counts over larger sky areas is in progress (Machalski & Jamrozy, in preparation).

6.4. Redshift distributions

Complete redshift data of a given sample of radio sources are highly required for calculations of their intrinsic power, linear size, etc. Such data are also crucial for the observational verification of cosmological evolutionary models. Unfortunately, completing spectroscopic redshift content of most of the flux-limited samples is very difficult for the

well known reasons. However, for some objects, e.g. elliptical radio galaxies, redshift can be reliably estimated from their apparent magnitude (especially K mag) and/or angular size. The latter method was used by Vigotti et al. (1989) to estimate galaxy redshifts in the B3-VLA sample.

In this paper, another possibility of estimating a *redshift distribution* of the subsamples of FRII sources is employed. The estimation is based on the empirical correla-

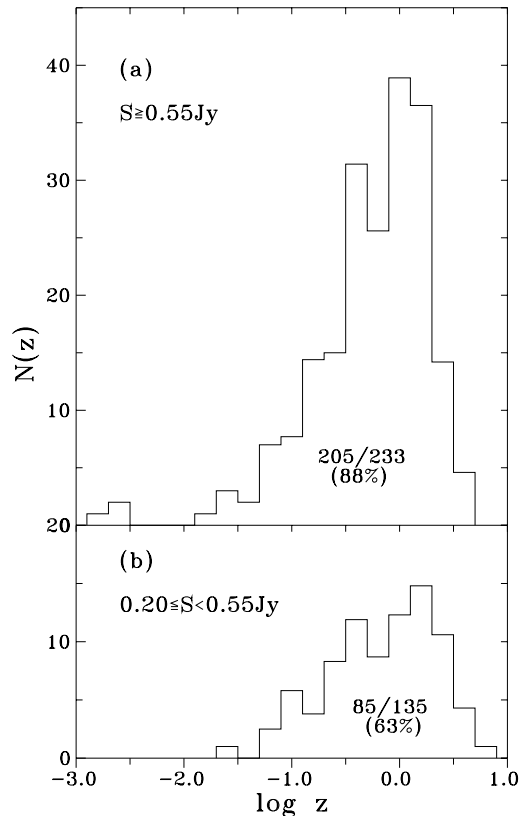


Fig. 5. Estimated redshift distributions of sources: **a)** in Subsample 1; **b)** in Subsample 2+3. The fraction of redshifts measured and/or estimated in each Subsample is given

tion between the power and surface brightness ($\log P$ vs. $\log B$) of FRII-type sources; the latter parameter being dependent on the apparent flux density and angular separation between hot spots in their lobes. It can be shown (Machalski, in preparation) that for a given $\log P$ (a range of $\log B$, in practice), the distribution of $\log P$ has a definite functional form. Therefore, for each FRII source in a sample one can calculate the probability of having $\log P$ in a certain power range (bin), and hence a redshift range. A sum of these probabilities in each redshift range, divided by the number of sources involved, gives the normalised distribution of redshift. If the sample is unbiased (the implicit assumption about random sampling of the redshift is present), the estimated z -distribution is statistically

Table A1. Gaussian models for the added sources. The components are fitted to our own, or FIRST [d+dd], or NVSS [C+P] VLA maps

GB/GB2 name	R.A. (J2000)	Decl. (J2000)	$S_{1.4}$ [mJy]	Comp. size ["] × ["]	PA [°]	LAS ["]	OPA [°]	VLA map
0753+360	07 56 21.56 21.98	+35 54 43.0 41.0	20 4 20 8	2.8 × 1.9 3.0 × 1.9	13 8 11 3	8.3	11 1	07570+36
0753+373 <i>opt.</i>	07 56 28.26 28.26	+37 14 55.8 53.0	23 6	1.5 × 0.8	3 5	–	–	07570+37
0754+368 <i>opt.</i>	07 57 51.29 52.63 53.82 53.34	+36 39 33.6 40 12.5 40 42.2 40 19.6	13 0 5 16 2	43 × 19 45 × 11	1 6 – 7	> 76	2 4	C0806P36
0809+503 <i>opt.</i>	08 13 17.11 20.55 18.90	+50 12 29.1 47.1 41.9	22 5 34 3	19 × 14 19 × < 13	6 2 5 3	47	6 1	C0824P52
0813+379	08 16 44.52 45.01	+37 49 12.1 20.1	13 1 19 0	3.3 × 1.3 4.1 × 1.2	2 5 4 2	12	12 6	08150+37
0820+367	08 23 47.83 48.62	+36 32 51.6 31.1	18 0 7 4	1.6 × 0.7 3.0 × 1.5	13 9 0	23	15 6	08240+36
0922+322	09 25 32.73	+31 59 52.9	53 1	3.6 × 1.4	16 6	–	–	09240+32
0958+346 <i>opt.</i>	10 01 11.92 11.95	+34 24 50.4 49.5	20 3	0.6 × 0.3	2 9	< 1.2	–	own
1042+392	10 45 14.67 15.40	+38 56 39.8 36.7	31 6 35 0	2.3 × 0.8 1.9 × 1.0	6 5 8 5	11	9 6	own
1127+348	11 30 04.95 06.57	+34 34 40.6 24.3	9 5 10 2	24 × 15 19 × 13	13 0 17 7	35	12 7	11300+34
1420+326 <i>opt.</i>	14 22 30.38 30.35	+32 23 10.4 10.0	40 8	1.3 × 1.0	1 8	–	–	14210+32
1550+346	15 52 50.59	+34 30 16.3	19 5	1.2 × 1.1	9 0	–	–	15510+34
1619+378 <i>opt.</i>	16 21 11.29 11.43	+37 46 04.9 04.7	62 7	1.0 × 0.8	5 5	–	–	16210+37

consistent with the distribution of true, spectroscopic redshift.

Using this method, the redshift distributions obtained for 88 per cent of the sources in Subsample 1 is shown in Fig. 5a. The sources for which the redshift cannot be estimated are exclusively compact ones and mostly optically unidentified. Similarly, the estimated redshift distribution for 63 per cent of the sources in Subsamples 2 and 3 is shown in Fig. 5b. These distributions suggest that about 8–10 FR II-type sources in our sample can be expected at redshift $z > 3$. The number of objects above this redshift may be even greater if the unidentified compact sources (especially CSS ones) are taken into account.

Appendix

This Appendix contains additional 1400-MHz and 4885-MHz VLA maps of some sources from the original sample, and numerical data of those sources included

in the revised sample which are adequately described by Gaussian component fits to the VLA images.

Figure A1 shows the 4885-MHz maps of central regions of six but one radio galaxies from Table 4. The maps resolution (FWHM of the restoring beam) is about 0.5 arcsec. Two of these galaxies (0912+489 and 1104+365) have FR II morphology with unresolved radio cores. The remaining (0838+325, 1059+351, 1141+466, and 1325+321) are classified as FR I type. In these latter sources, a radio core was detected in the 0838+325 galaxy only. The inner structure of this galaxy, of size of about 17 kpc, consists of two bright emitting regions extended symmetrically off the core. They resemble usual “hot spots” at the edge of classical double edge-brightened (FR II) structure, however the low-resolution 1.4-GHz VLA images of this source (Fanti et al. 1986; 1987) show very extended diffuse emission stretched out far away from these bright spots, and characteristic for edge-darkened sources. No trace of jets were detected. A similar inner

structure but without a pronounced core characterizes the galaxy 1141+466 as well. In turn, the brightest spots in an inner “S-shaped” structure of the galaxies 1059+351 and 1325+321 are evidently related to a base of twisted jets.

The inner part of the optically unidentified source 1348+352 is very enigmatic. The VLA 1465-MHz map (Machalski & Condon 1983b) showed the very bright central region suggesting a core-jet structure and a low-brightness extended emission. A twisted ridge could be seen in it. The reality of that emission is now confirmed due to the FIRST survey. A relevant image of the source (on the FIRST map 13510+35071) indicates that the dif-fused emission includes about 45 per cent of the total flux at 1400 MHz. Surprisingly, our VLA 4885-MHz map (Fig. A1) of the source’s central region with the angular resolution of about 0.5 arcsec does not show a typical core structure. The 3×2.5 arcsec region reveals a “hot spot” at its westernmost side and a ring-like emission towards the east. This “hot spot” with a deconvolved size of 0.7×0.6 arcsec has a spectral index between 1.4 and 5 GHz, $\alpha_{1.4}^5 \approx 0.67 \pm 0.06$. It is flatter than the corresponding index of the central region, which has $\alpha_{1.4}^5 = 0.84 \pm 0.04$. The extended diffuse emission has exactly the same index of 0.84. Consequently, the source 1348+352 is probably of FRI type, with twisted structure characteristic for precessing jets but strongly projected onto the sky.

The correct 1400-MHz map of the galaxy 0910+353, reproduced from the FIRST 09120+35 map is shown in Fig. A2. Parameters of the Gaussian components fitted by the least-square method to VLA images of the sources added to the revised sample, and the sky coordinates of the identified optical objects (cf. Table 3), are given in Table A1. If these fits were taken from the FIRST or NVSS maps, this is noted in Table A1 by the number of original VLA map.

References

- Allington-Smith J.R., Perryman M.A.C., Longair M.S., Gunn J.E., 1982, MNRAS 201, 331
- Allington-Smith J.R., Spinrad H., Djorgovski S., Liebert J., 1988, MNRAS 234, 1091
- Andernach H., Waldthausen H., Wielebinski R., 1980, A&AS 41, 339
- Antonucci R.R.J., 1985, ApJS 59, 499
- Baars J.W.M., Genzel R., Pauliny-Toth I.I.K., Witzel A., 1977, A&A 61, 99
- Becker R.H., White R.L., Helfand D.J., 1995, ApJ 450, 559
- Benn C.R., Grueff G., Vigotti M., Wall J.V., 1982, MNRAS 200, 747
- Burbidge E.M., 1970, ApJ 160, L33
- Burbidge E.M., Strittmatter P.A., 1972, ApJ 172, L37
- Burns J.O., Schwendeman E., White R.A., 1983, ApJ 271, 575
- Capetti A., Morganti R., Parma P., Fanti R., 1993, A&AS 99, 407
- Colla G., Fanti C., Fanti R., et al., 1972, A&AS 7, 1
- Colla G., Fanti C., Fanti R., et al., 1973, A&AS 11, 291
- Cohen A.M., Porcas R.W., Browne I.W.A., Daintree E.J., Walsh D., 1977, MmRAS 84, 1
- Condon J.J., 1983, ApJS 53, 459
- Condon J.J., 1984, ApJ 287, 461
- Condon J.J., Broderick J.J., 1985, AJ 90, 2540
- Condon J.J., Broderick J.J., 1988, AJ 96, 30
- Condon J.J., Broderick J.J., Seielstad, G.A., 1989, AJ 87, 1064
- Condon J.J., Cotton W.D., Greisen E.W., et al., 1996, NCSA Astr. Dig. Image Lib.
- Cousins A.W.J., 1976, MmRAS 81, 25
- Crawford C.S., Fabian A.C., 1996, MNRAS 282, 1483
- deRuiter H.R., Parma P., Fanti C., Fanti R., 1986, A&AS 65, 111
- Dixon R.S., Kraus J.D., 1968, AJ 73, 381
- Djorgovski S.G., Thompson D.J., Vigotti M., Grueff G., 1990, PASP 102, 113
- Douglas J.N., Bash F.N., Torrence G.W., Wolfe C., 1980, Univ. of Texas, Prep. No. 17
- Dunlop J.S., Peacock J.A., 1990, MNRAS 247, 19
- Fanaroff B.J., Riley J.M., 1974, MNRAS 167, 31P
- Fanti C., Fanti R., Gioia I.M., et al., 1977, A&AS 29, 279
- Fanti C., Fanti R., deRuiter H.R., Parma P., 1986, A&AS 65, 145
- Fanti C., Fanti R., deRuiter H.R., Parma P., 1987, A&AS 69, 57
- Fey AL., Clegg A.W., Fomalont E.B., 1996, ApJS 105, 299
- Ficarra A., Grueff G., Tomassetti G., 1985, A&AS 59, 255
- Ford H., Crane P., Jacoby G.H., Lawrie D.G., van der Hulst J.M., 1985, ApJ 293, 132
- Gioia I.M., Fabbiano G., 1987, ApJS 63, 771
- Gower J.F.R., Scott P.F., Wills D., 1967, MmRAS 71, 49
- Gregory P.C., Scott W.K., Douglas K., Condon J.J., 1996, ApJS 103, 427
- Griffith M., Langston G., Heflin M., Conner S., Burke B., 1991, ApJS 75, 801
- Grueff G., Vigotti M., 1979, A&AS 35, 371
- Grueff G., Vigotti M., Spinrad H., 1980, A&A 86, 50
- Hales S.E.G., Baldwin J.E., Warner P.J., 1993, MNRAS 263, 25
- Haslam C.G.T., Kronberg P.P., Waldthausen H., Wielebinski R., 1978, A&AS 31, 99
- Henstock D.R., Browne I.W.A., Wilkinson P.N., et al., 1995, ApJS 100, 1
- Henstock D.R., 1995 (priv. info.)
- Hewitt A., Burbidge G., 1993, ApJS 87, 451 (QSO cat.)
- Hook I.M., MaMahon R.G., Irwin M.J., Hazard C., 1996, MNRAS 282, 1274
- Huchra J., Davis M., Latham D., Tonry J., 1983, ApJS 52, 89
- Hughes P.A., Aller H.D., Aller M.F., 1992, ApJ 396, 469
- Hummel E., Pedlar A., van der Hulst J.M., Davies R.D., 1985, A&AS 60, 293
- Jaffe W., Perola G.C., 1974, A&A 31, 223
- Johnson H.L., 1966, ARA&A 4, 193
- Katgert J.K., 1978, A&AS 31, 409
- Katgert P., Katgert-Merkelijn J.K., LePoole R.S., van der Laan H., 1973, A&A 23, 171
- Katgert-Merkelijn J., Lari C., Padrielli L., 1980, A&AS 40, 91
- Kulkarni V.K., 1978, MNRAS 185, 123
- Kühr H., Nauber U., Pauliny-Toth I.I.K., Witzel A., 1981, A&AS 45, 367

- LaHulla J.F., Merighi R., Vettolani G., Vigotti M., 1991, *A&AS* 88, 525
- Laing R.A., Riley J.M., Longair M.S., 1983, *MNRAS* 204, 151
- Langston G.I., Hefflin M.B., Conner S.R., et al., 1990, *ApJS* 72, 621
- Leahy J.P., Perley R.A., 1991, *AJ* 102, 537
- Lilly S.J., Longair M.S., Allington-Smith J.R., 1985, *MNRAS* 215, 37
- Lousdale C.J., Barthel P.D., Miley G.K., 1993, *ApJS* 87, 63
- Machalski J., 1978a, *Acta Astr.* 28, 367
- Machalski J., 1978b, *A&A* 65, 157
- Machalski J., 1988, *Acta Astr.* 38, 163
- Machalski J., 1991, *Acta Astr.* 41, 39
- Machalski J., 1992, *Acta Astr.* 42, 335
- Machalski J., 1996, in “Extragalactic Radio Sources” (IAU Symp. No. 175), Ekers R. et al. (ed.). Kluwer Acad. Pub., p. 545
- Machalski J., Brandt W.N., 1996, *MNRAS* 282, 1305
- Machalski J., Condon J.J., 1983a, *AJ* 88, 143 (Paper III)
- Machalski J., Condon J.J., 1983b, *AJ* 88, 1591 (Paper IV)
- Machalski J., Condon J.J., 1985a, *AJ* 90, 5 (Paper V)
- Machalski J., Condon J.J., 1985b, *AJ* 90, 973
- Machalski J., Condon J.J., 1986, *AJ* 91, 998
- Machalski J., Condon J.J., 1990, *PASP* 102, 53
- Machalski J., Engels D., 1994, *MNRAS* 266, L69
- Machalski J., Inoue M., 1990, *MNRAS* 243, 209
- Machalski J., LaFranca F., 1988, *IAU Circ. No. 4573*
- Machalski J., Magdziarz P., 1993a, *A&A* 267, 363
- Machalski J., Magdziarz P., 1993b, *A&AS* 102, 315
- Machalski J., Maslowski J., 1982, *AJ* 87, 1132 (Paper I)
- Machalski J., Maslowski J., Condon J.J., Condon M.A., 1982, *AJ* 87, 1150 (Paper II)
- Machalski J., Wiśniewski W.Z., 1988, *MNRAS* 231, 1065
- Maslowski J., 1972, *Acta Astr.* 22, 227
- Maslowski J., Kellermann K.I., 1988, *AJ* 95, 1659
- Maxfield L., Thompson D., Djorgovski S., et al., 1995, *PASP* 107, 369
- Moles M., Garcia-Pelayo J.M., Masegosa J., Aparicio A., Quintana J.M., 1985, *A&A* 152, 271
- Morabito D.D., Niell A.E., Preston R.A., et al., 1986, *AJ* 91, 1038
- Morganti R., Ulrich M.H., Tadhunter C.N., 1992, *MNRAS* 254, 546
- Morganti R., Killeen N.E.B., Tadhunter C.N., 1993, *MNRAS* 263, 1023
- Netzer H., Heller A., Loinger F., et al., 1996, *MNRAS* 279, 429
- O’Donoghue A.A., Eilek J.A., Owen F.N., 1993, *ApJ* 408, 428
- Owen F.N., Condon J.J., Ledden J.E., 1983, *AJ* 88, 1
- Owen F.N., Puschell J.J., 1984, *AJ* 89, 932
- Owen F.N., White R.A., Thronson H.A., 1988, *AJ* 95, 1
- Parma P., deRuiter H.R., Fanti C., Fanti R., 1986, *A&AS* 64, 135
- Pauliny-Toth I.I.K., Wade C.M., Heeschen D.S., 1966, *ApJS* 13, 65
- Peacock J.A., Miller L., Longair M.S., 1986, *MNRAS* 218, 265
- Pearson T.J., Readhead A.C.S., 1988, *ApJ* 328, 114
- Perley R.A., 1982, *AJ* 87, 859
- Perley R.A., Fomalont E.B., Johnston K.J., 1980, *AJ* 85, 649
- Perley R.A., Fomalont E.B., Johnston K.J., 1982, *ApJ* 255, L93
- Petrosian V., Dickey J., 1973, *ApJ* 186, 403
- Pilkington J.D.H., Scott P.F., 1965, *MmRAS* 69, 183
- Polatidis A.G., Wilkinson P.N., Xu W., et al., 1995, *ApJS* 98, 1
- Porcas R.W., Urry C.M., Browne I.W.A., et al., 1980, *MNRAS* 191, 607
- Reid A., Shone D.L., Akujor C.E., et al., 1995, *A&AS* 110, 213
- Rioja M.J., Porcas R.W., Machalski J., 1996, *Proc. IAU Symp. No. 175 “Extragalactic Radio Sources”*, Ekers R. et al. (ed.). Kluwer Acad. Pub., p. 122
- Rudnick L., Owen F.N., 1977, *AJ* 82, 1
- Ryś S., Machalski J., 1990, *A&A* 236, 15
- Sandage A., 1972, *ApJ* 178, 25
- Sandage A., Kristian, J., Westphal, J.A., 1976, *ApJ* 205, 688
- Sanghera H.S., Saikia, D.J., Lüdke, E., et al., 1995, *A&A* 295, 629
- Sargent W.L.W., 1973, *ApJ* 182, L13
- Seielstad G.A., Pearson T.J., Readhead A.C.S., 1983, *PASP* 95, 842
- Smith H.E., Spinrad H., 1980, *PASP* 92, 553
- Spinrad H., 1982, *PASP* 94, 397
- Spinrad H., Djorgovski S.G., 1984, *ApJ* 285, L49
- Spinrad H., Filippenko A.V., Wyckoff S., et al., 1985, *ApJ* 299, L7
- Stickel M., Kühr H., 1994, *A&AS* 105, 67
- Strittmatter P.A., Carswell R.F., Gilbert G., Burbidge E.M., 1974, *ApJ* 190, 509
- Strom S.E., Riley J.M., Spinrad H., et al., 1990, *A&A* 227, 19
- Tadhunter C.N., Morganti R., di Serego Alighieri S., Fosbury R.A.E., Danziger I.J., 1993, *MNRAS* 263, 999
- Thakkar D.D., Xu W., Readhead A.C.S., et al., 1995, *ApJS* 98, 33
- Thompson D., Djorgovski S., Vigotti M., Grueff G., 1992, *ApJS* 81, 1
- Vallée J.P., Wilson A.S., 1976, *Nat* 259, 451
- Vallée J.P., Bridle A.H., Wilson A.S., 1981, *ApJ* 250, 66
- Valtaoja E., Teräsanta H., Urpo S., et al., 1992, *A&A* 254, 80
- van Albada G.D., van der Hulst J.M., 1982, *A&A* 115, 263
- Véron-Cetty M.P., Véron P., 1993, *ESO Sci. Report No. 13*
- Vermeulen R.C., Taylor G.B., Readhead A.C.S., Browne I.W.A., 1996, *AJ* 111, 1013
- Vigotti M., Grueff G., Perley R., Clark B.G., Bridle A.H., 1989, *AJ* 98, 419
- Waldthausen H., Haslam C.G.T., Wielebinski R., Kronberg P.P., 1979, *A&AS* 36, 237
- Wall J.V., Peacock J.A., 1985, *MNRAS* 216, 173
- Walsh D., Wills B.J., Wills D., 1979, *MNRAS* 189, 667
- Warner P.J., Riley J.M., Eales S.A., Downes A.J.B., Baldwin J.E., 1983, *MNRAS* 204, 1279
- White R.L., Becker R.H., 1992, *ApJS* 79, 331
- Wilkes B.J., Tananbaum H., Worrall D.M., et al., 1994, *ApJS* 92, 53
- Windhorst R.A., Miley G.K., Owen F.N., Kron R.G., Koo D.C., 1985, *ApJ* 289, 494
- Wilkinson A., Hine R.G., Sargent W.L.W., 1981, *MNRAS* 196, 669
- Worrall D.M., Wilkes B.J., 1990, *ApJ* 360, 396
- Xu W., Reahead A.C.S., Pearson T.J., Polatidis A.G., Wilkinson P.N., 1995, *ApJS* 99, 297
- Zwicky F., Herzog E., 1963, “Catalogue of Galaxies and Clusters of Galaxies”, Caltech (ed.), Pasadena

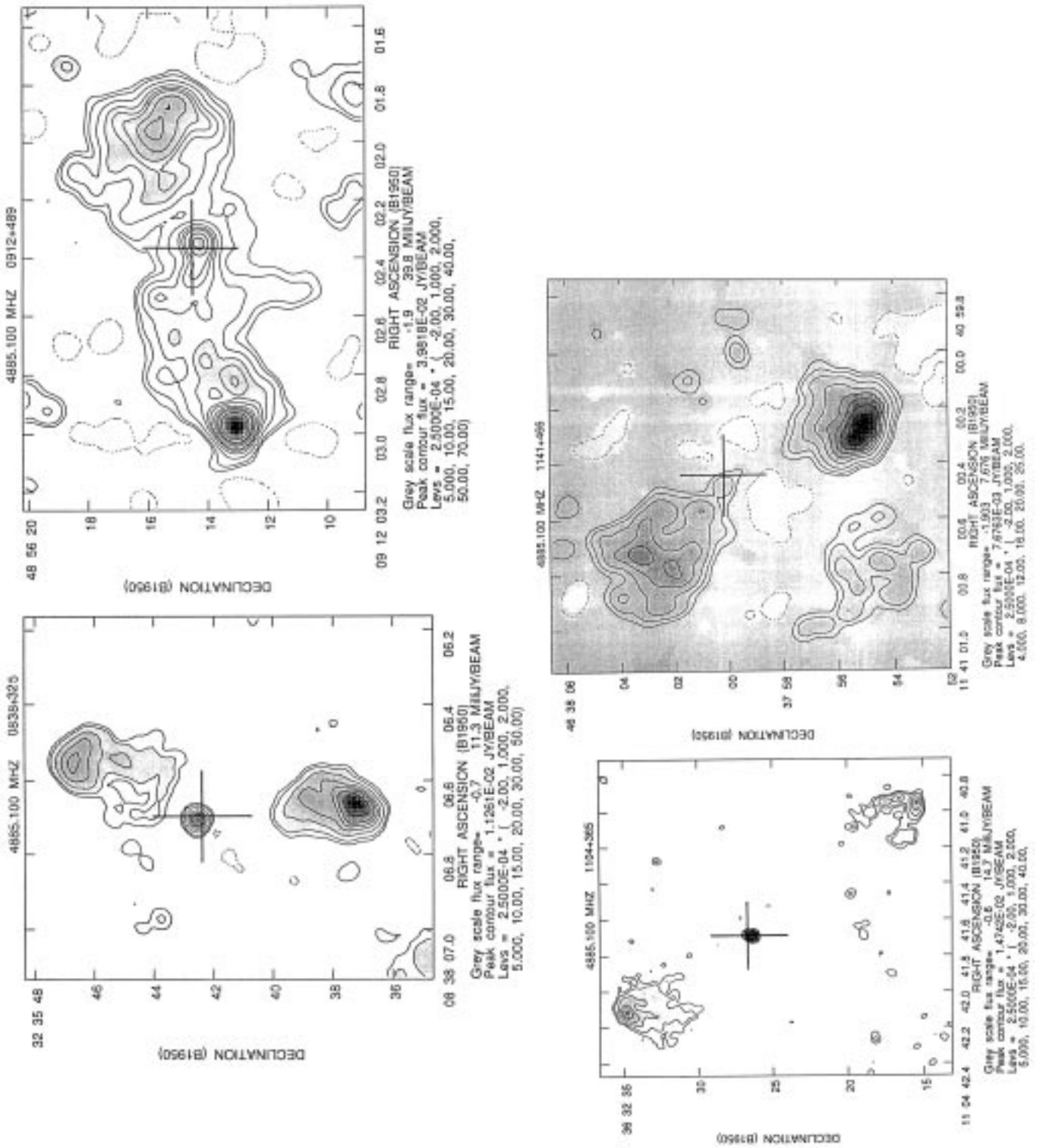


Fig. A1. VLA 4885-MHz contour maps of the sources selected from the revised GB/GB2 sample. FWHB of the restoring beam is 0.55×0.50 arcsec. The contour levels are shown under each map. The best optical positions of the center of identified galaxies are marked by the large crosses

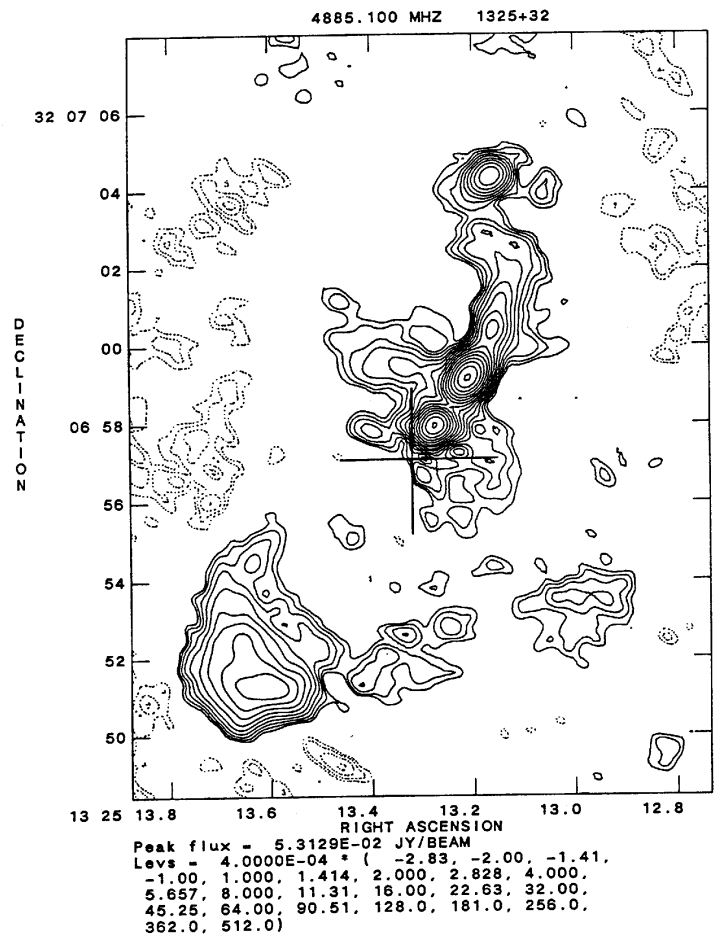
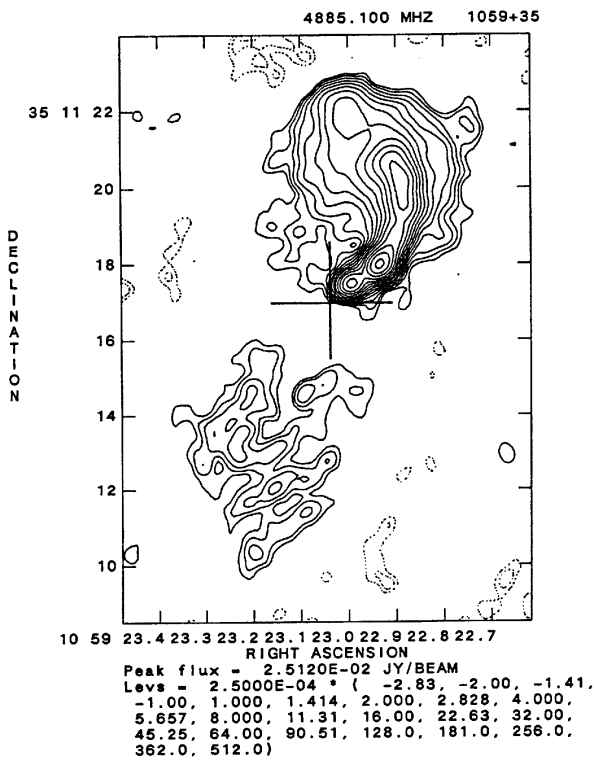
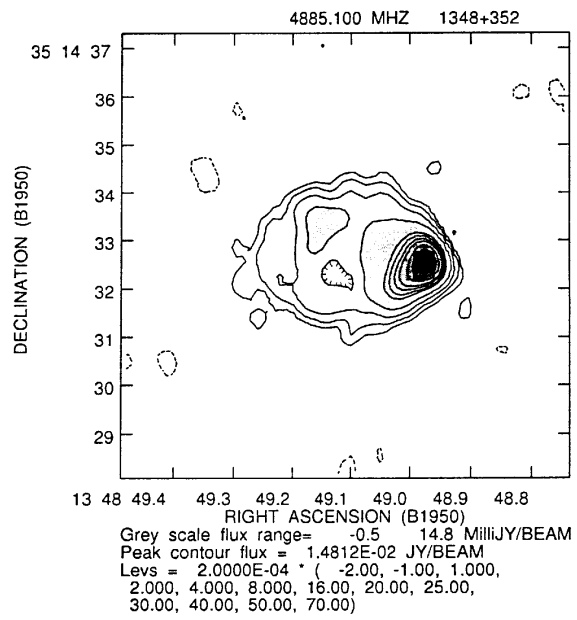


Fig. A1. continued

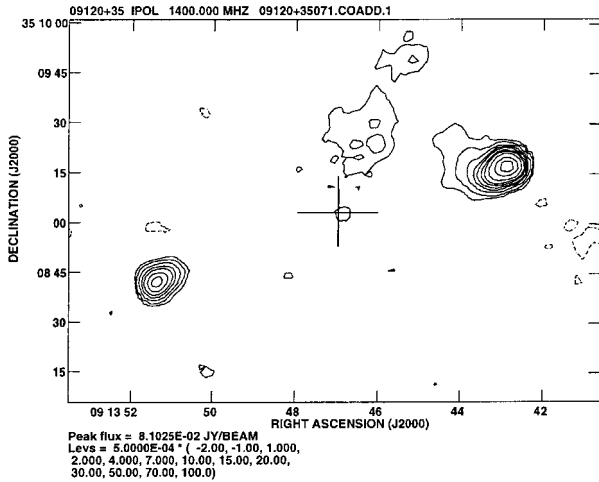


Fig. A2. VLA 1400-MHz contour map of the source 0910+353 reproduced from the FIRST 09120+35 map (courtesy of R. Becker). FWHB of the restoring beam is 5.4×5.4 arcsec. The contour levels are shown under the map. The position of the optical galaxy is marked by the cross

Notes to individual sources in Table 3

0717+367: in Abell cluster 579

0722+393: Confusing, flat-spectrum, possibly variable source at $07^{\text{h}}26^{\text{m}}04^{\text{s}}.8$; $+32^{\circ}12'28''$ (5.8 arcmin away). $S_{1.4} \approx 135 - 210$ mJy.

0723+488: A featureless optical spectrum was observed in March 1992 with the Asiago 182-cm telescope (cf. Machalski 1992). Variable in the radio (cf. Table 3) and likely in the optical.

0751+485: A featureless optical spectrum was observed in March 1992 with the Asiago 182-cm telescope (cf. Machalski 1992).

0755+379: NGC 2484; UGC 4125. References to WSRT maps and physical parameters in Condon & Broderick (1988).

0755+480A: Confusing, extended, double source 0755+480B (3.0 arcmin away), identified with a faint galaxy.

0804+499A: 8.4 arcmin apart from very compact variable quasar 0804+499B.

0804+370: Confusing source at $08^{\text{h}}08^{\text{m}}29^{\text{s}}.44$; $+36^{\circ}59'43''.7$, $S_{1.4} \approx 60$ mJy.

0809+328: The radio source is likely associated with one of two close (separation of 2.3 arcsec) galaxies in a pair.

0810+351: Centroid of the double radio source coincides well with the bright elliptical galaxy, however morphological type of the source with evident bright “hot spots” is not typical for galaxies at $z < 0.1$.

0816+367: Confusing flat-spectrum source at $08^{\text{h}}20^{\text{m}}20^{\text{s}}.2$; $+36^{\circ}40'05''$ (4.5 arcmin away). $S_{1.4} \approx 100$ mJy.

0818+472: Two confusing sources: $S_{1.4} \approx 190$ mJy at $08^{\text{h}}21^{\text{m}}59^{\text{s}}.0$; $+47^{\circ}02'53''$ (5.2 arcmin away), and $S_{1.4} = 54$ mJy, flat-spectrum, at $08^{\text{h}}22^{\text{m}}09^{\text{s}}.6$; $+47^{\circ}05'53''$ (6.9 arcmin away).

0822+394: The spectrum breaks at about 1.4 GHz. Low- and high-frequency spectral indices differ significantly: $\alpha_{0.4}^{1.4} \approx 0.42$, $\alpha_{1.4}^{10} \approx 1.14$.

0829+512: Neither of two suggested galaxy identifications (cf. Paper III) is convincing, however association of the radio source with a faint distant galaxy is very probable.

0838+325: in Abell cluster 694/695. 4885-MHz VLA map of the central part of the source is shown in Fig. A1 (Appendix).

0844+319: IC 2402 galaxy.

0906+480A: Close pair (4.3 arcmin apart) with 0906+480B. Both are very compact; deconvolved size of 0.0×0.0 arcsec at 5 GHz. Spectral indices quoted in Paper IV and Machalski & Inoue (1990) were erroneously interchanged. Probably variable above 5 GHz.

0908+380: Confusing, steep-spectrum source (0908+380B in the B3VLA sample; Vigotti et al. 1989) at $09^{\text{h}}11^{\text{m}}48^{\text{s}}.5$; $+37^{\circ}50'19''$ (3.1 arcmin away). $S_{1.4} \approx 150$ mJy.

0910+353: The VLA A-array map and optical identification of the source published in Paper IV were wrong. The correct map reproduced from the FIRST survey (courtesy of R.H. Becker) with the new identification indicated is shown in Fig. A2 (Appendix).

0911+354: Northern component with $S_{1.4} \approx 50$ mJy (cf. VLA A-array map in Paper IV) may be a separate source.

0918+381: Confusing, very steep-spectrum, double source 0919+381 at $09^{\text{h}}22^{\text{m}}15^{\text{s}}.20$; $+37^{\circ}54'03''$ (6.9 arcmin away). $S_{1.4} = 295 \pm 6$ mJy.

0927+352: Radio, optical, and X-ray properties of the source are discussed in Machalski & Brandt (1996).

0928+480: Southern component at $09^{\text{h}}31^{\text{m}}34^{\text{s}}.3$; $+47^{\circ}49'47''$ (marked “B” in Paper II) is likely a separate source. $S_{1.4} = 186$ mJy in NVSS.

0949+354: Confusing, flat-spectrum source at $09^{\text{h}}52^{\text{m}}22^{\text{s}}.6$; $+35^{\circ}08'03''$ (5.2 arcmin away). $S_{1.4} \approx 50$ mJy.

0954+346: Confusing, steep-spectrum source at $09^{\text{h}}57^{\text{m}}48^{\text{s}}.3$; $+34^{\circ}17'28''$ (4.8 arcmin away). $S_{1.4} \approx 90$ mJy

0955+320: Confusing, steep-spectrum source at $09^{\text{h}}58^{\text{m}}25^{\text{s}}.37$; $+31^{\circ}47'17''.2$ (7.1 arcmin away). $S_{1.4} \approx 170$ mJy

1003+484: 3C 235. The spectrum breaks at about 320 MHz. $\alpha_{0.38}^{0.4} \approx 0.82$, $\alpha_{0.4}^{15} \approx 1.16$.

1014+397: The optical magnitudes are for the galaxy at $10^{\text{h}}17^{\text{m}}18^{\text{s}}.60$; $+39^{\circ}31'19''.3$ (cross “1” in

Paper II). Vigotti et al. (1989) identified this extended double source with another brighter galaxy at $10^{\text{h}}17^{\text{m}}17^{\text{s}}.86; +39^{\circ}31'46''.5$. Thompson et al. (1992) determined it as a NLRG with the redshift of 0.089.

1017+487: in Abell cluster 1003.

1049+384: The optical spectrum shows intermediate properties between galaxies and quasars (Allington-Smith et al. 1988).

1104+365: The optical spectrum as above.

1127+507: Confusing steep-spectrum source $1126+506$ at $11^{\text{h}}29^{\text{m}}12.^{10}; +50^{\circ}23'35''$ (6.1 arcmin away). $S_{1.4} \approx 348$ mJy.

1129+351: The optical spectrum shows intermediate properties between galaxies and quasars (Allington-Smith et al. 1988).

1131+493: UGC 6549; IC 708; in Abell cluster 1314. References to WSRT maps and physical parameters in Condon & Broderick (1988).

1132+492: IC 711; in Abell cluster 1314. Low-resolution Effelsberg map at 2.7 GHz in Haslam et al. (1978).

1141+466: in Abell cluster 1361. Low-resolution Effelsberg map at 2.7 GHz in Waldhausen et al. (1979). Confusing, flat-spectrum source at $11^{\text{h}}43^{\text{m}}10^{\text{s}}.9; +46^{\circ}23'40''$ (5.5 arcmin away). $S_{1.4} \approx 190$ mJy. For its low-resolution maps cf. Rudnick & Owen (1977) and Andernach et al. (1980). 4885-MHz VLA map of central part of the source is shown in Fig. A1 (Appendix).

1144+352: A total extent of the radio emission of about 10 arcmin (about 990 kpc) is suggested from the 4.85-GHz map N111200W of Condon et al. (1989). Its position angle (PA) of about 105 deg is compatible with PA = 118° of a two-sided, about 45 kpc extended, emission from the very compact and bright core on the map 11480+35071B of Becker et al. (1995). Moreover, the VLBI-scale structure (about 22 mas, corresponding to about 37 pc) observed by Henstock et al. (1995), has PA = 121°5.

1144+497: Confusing source at $11^{\text{h}}47^{\text{m}}50^{\text{s}}.2; +49^{\circ}28'05''$ (4.1 arcmin away). $S_{1.4} \approx 80$ mJy. Though the blue optical object lies on the overall axis of this double source, the identification is not convincing.

1151+384: Bright, confusing, steep-spectrum double source $1151+383$ at $11^{\text{h}}54^{\text{m}}01^{\text{s}}.2; +38^{\circ}05'07''$ (6.9 arcmin away). $S_{1.4} \approx 500$ mJy.

1152+462: Confusing source $1152+463$ at $11^{\text{h}}54^{\text{m}}43^{\text{s}}.95; +46^{\circ}01'32''.4$ (7.5 arcmin away). $S_{1.4} = 217 \pm 10$ mJy Designated as 1152+462B in Paper V).

1158+345: The optical identification is not certain.

1202+499B: Confusing source $1202+499A$ (3.0 arcmin away). $S_{1.4} = 154$ mJy.

1216+475: M 106; NGC 4258; UGC 7353. Low-luminosity, starburst galaxy with a trace of non-thermal nucleus. References to WSRT and Effelsberg maps, as well as physical parameters in Condon & Broderick (1988).

1218+489: Though the blue optical object lies on overall axis of this source (cf. Paper IV), the identification may be an accidental one.

1226+492: Confusing, flat-spectrum source at $12^{\text{h}}28^{\text{m}}52^{\text{s}}.9; +49^{\circ}04'36''$ (6.6 arcmin away). $S_{1.4} \approx 50$ mJy.

1230+486: Very likely variable at frequencies above 5 GHz. Confusing steep-spectrum source at $12^{\text{h}}32^{\text{m}}35^{\text{s}}.7; +48^{\circ}16'50''$ (4.7 arcmin away) identified with 4C 48.35. $S_{1.4} \approx 150$ mJy.

1231+495: Faint red optical object at $12^{\text{h}}34^{\text{m}}20^{\text{s}}.61; +49^{\circ}14'18''.7$ (cf. Paper IV) might be associated with this double radio source.

1237+353: Confusing, compact, steep-spectrum source at $12^{\text{h}}40^{\text{m}}19^{\text{s}}.2; +34^{\circ}56'39''$ (6.4 arcmin away). $S_{1.4} \approx 190$ mJy.

1239+328: NGC 4631; UGC 7865. Low-luminosity star-burst galaxy. References to WSRT, NRAO interferometer, and Effelsberg maps, as well as physical parameters in Condon & Broderick (1988).

1248+350: Deep observations of the field at 408 MHz (5C12 survey: Benn et al. 1982), at 610 and 1415 MHz (WSRT surveys: Katgert 1978; Katgert et al. 1973, respectively). Identified with 5C 12.2 and 1248+35W1. Confusing, faint, double source (5C 12.4; 1248+34W1) at $12^{\text{h}}50^{\text{m}}46^{\text{s}}.0; +34^{\circ}39'59''$ (4.7 arcmin away). $S_{1.4} \approx 90$ mJy.

1249+508: 3C 277. The spectrum breaks at about 1.1 GHz. $\alpha_{0.15}^{1.1} \approx 0.90$, $\alpha_{1.1}^{1.0} \approx 1.18$.

1256+489: 4C 48.36. Confusing, steep-spectrum source at $12^{\text{h}}59^{\text{m}}42^{\text{s}}.4; +48^{\circ}43'22''$ (5.4 arcmin away). $S_{1.4} \approx 110$ mJy.

1322+366: NGC 5141; UGC 8433. WSRT 5-GHz map in Fanti et al. (1977). Physical parameters in Condon & Broderick (1988).

1324+498A: Confusing, flat-spectrum source $1324+498B$ at $13^{\text{h}}26^{\text{m}}39^{\text{s}}.3; +49^{\circ}33'55''$ (4.1 arcmin away). $S_{1.4} \approx 90$ mJy.

1327+474: M 51; NGC 5194; UGC 8493. Low-luminosity star-burst galaxy with faint non-thermal radio core. References to WSRT and Effelsberg maps, as well as physical parameters in Condon & Broderick (1988). The spectrum breaks at about 1.4 GHz. $\alpha_{0.038}^{1.4} \approx 0.67$, $\alpha_{1.4}^5 \approx 1.07$.

1329+503: Confusing, steep-spectrum source at $13^{\text{h}}30^{\text{m}}56^{\text{s}}.4; +50^{\circ}09'04''$ (6.7 arcmin away). $S_{1.4} \approx 200$ mJy.

1348+352: Unique radio source; a more detailed discussion in the Appendix.

1354+325: For a discussion of the optical field, cf. Machalski & Condon (1985b).

1413+349: Confusing, steep-spectrum source at $14^{\text{h}}16^{\text{m}}17^{\text{s}}.2; +34^{\circ}48'05''$ (4.4 arcmin away). $S_{1.4} \approx 130$ mJy.

1415+463: 4C46.29. Confusing source 1414+463 at $14^{\text{h}}16^{\text{m}}42^{\text{s}}.9; +46^{\circ}03'04''$ (6.0 arcmin away). $S_{1.4} \approx 140$ mJy.

1452+502A: Close pair (2.5 arcmin apart) with compact quasar 1452+502B. All flux densities in the surveys given in Col. 2 are strongly confused.

1504+346: in Abell cluster 2025.

1507+476: The optical galaxy is 2.1 arcsec apart from this compact radio source whose observed structure was deconvolved into two “point” components separated by 0.87 arcsec (Paper III).

1527+349: For a discussion of the optical field cf. Paper III.

1546+487: Confusing, steep-spectrum source at

$15^{\text{h}}47^{\text{m}}40^{\text{s}}.4; +48^{\circ}39'22''$ (7.1 arcmin away). $S_{1.4} \approx 220$ mJy.

1613+345: Two confusing sources at $16^{\text{h}}15^{\text{m}}39^{\text{s}}.2; +34^{\circ}21'57''$ and $16^{\text{h}}15^{\text{m}}44^{\text{s}}.5; +34^{\circ}21'15''$ (4.8 and 6.1 arcmin away, respectively), was recorded as 1613+344 in Owen et al. (1983) with a total flux $S_{1.4} \approx 70$ mJy.

1615+351: NGC 6109; UGC 10316. References to WSRT maps, and physical parameters in Condon & Broderick (1988).

1626+396: NGC 6166; UGC 10409. WSRT 1.4 and 5 GHz maps in Jaffe & Perola (1974). Physical parameters in Condon & Broderick (1988).

1636+379: in Abell cluster 2214.

Table 3. continued

0910+353	**//?//**	3	234 ± 26	0.79 ± .03	s	II	110	1.4A,B	0910+353	GAL (0.28)	18.2	20.1	0.09 13 46.90	+35 09 02.2 16	+
0911+354	**//?//**	2,3	282 ± 11	0.44 ± .06	c+	C(1s)	2.6	1.4A	0911+354	QSO 1.07	19.47	20.77	09 14 39.42	+35 12 04.6 16//591	+
0912+489	****//**	1,2	830 ± 26	0.83 ± .02	c-	II+cc	11.0	1.4A,4.9A	0912+489	GAL (0.60)	20.22		09 15 27.40	+48 43 43.5 15.32//54	
0913+391	****//**	1	1106 ± 24	0.41 ± .02	cpx	C(2s)	7.5	1.4A,(VLBI)	0913+391	QSO 1.269	19.59	<20.2	09 16 48.90	+38 54 28.2 15/40/53/67,85	
0914+349	****//**	1,2	853 ± 18	0.90 ± .02	c-	II	10.8	1.4A	0914+349	EF			09 17 16.38	+34 46 41.2 15	
0918+381	**//?//c**	1	[822]	0.99 ± .02	c-	II+cc	53	1.4P	0918+381	QSO 1.108	18.5	20.5	09 21 46.37	+37 54 07.0 14//67,85	+
0922+322	****//**	1	551 ± 33	0.86 ± .03	c-	II?	3.6	*	0922+322	EF			09 25 32.74	+31 59 53.2 Table A1	
0922+366	**//?//**	1	727 ± 28	0.81 ± .01	c-	I+cc	190	1.4B,B,C,C	0922+366	GAL 0.1117	15.60	17.99	09 25 39.05	+36 27 05.7 3.6,8,17//52/77	
0923+392	****//**	1	2666v(273)	(-0.4)	cpx	C(2s)	1.9	*(VLBI)	0923+392	XQSO 0.698	17.92		09 27 03.02	+39 02 20.9 /41,42,43/58/67,85/X2,X4	
0926+487	****//**	1,2	774 ± 24	0.85 ± .02	c-	CSS	2.6	1.4A	0926+487	GAL (0.45)	19.4	21.2	09 30 16.75	+48 31 46.0 15	
0927+362	****//**	1	1836 ± 42	0.89 ± .02	c-	II	7.7		0927+362	QSO 1.157	19.0	18.5	09 30 33.53	+36 01 24.8 ///85	
0927+352	**//?//**	2,3	475 ± 12	(0.6)	cpx	C(1s)	1.6	*(VLBI)	0927+352	XBL?	17.64v		09 30 55.28	+35 03 37.6 16/40/55//X5	+
0928+480	****//c**	1,2	559 ± 11	0.90 ± .02	c-	II	3.9	*	0928+480	NSO	18.7	19.7	09 31 31.93	+47 51 41.6 14	+
0929+327	****//**	1	688 ± 27	0.93 ± .02	c-	II	45	1.4P	0929+327	EF			09 32 34.58	+32 31 48.9 14	
0930+490	**//?//c**	2	379 ± 7	0.62 ± .03	c-	CSS	0.5	*	0930+490	EF			09 33 38.27	+48 50 06.2 16	
0930+493	**//?//**	1,2	721 ± 17	-0.03 ± .07	cpx	C	<0.4	*(VLBI)	0930+493	QSO 2.590	18.4	19.2	09 34 15.76	+49 08 21.7 15/40//66	
0936+345	**//?//**	2,3	268 ± 11	1.07 ± .04	c-	II	2.2	*	0936+345	EF			09 39 13.80	+34 16 46.8 16	
0936+361	**//?//**	1	3341 ± 48	0.78 ± .01	s	II+cc	306	1.4BC	0936+361	GAL 0.1368	16.08	18.35	09 39 52.74	+35 53 58.2 12//51/70	
0937+391	****//**	1	668 ± 19	0.93 ± .03	c-	II+cc	52	1.4P	0937+391	XQSO 0.618	18.5		09 41 03.87	+38 53 51.7 14//67,85/X4	
0938+485	****//**	2	310 ± 9	0.42 ± .06	cv	CSS	<0.4	*	0938+485	RO	22.58		09 41 27.89	+48 20 39.6 16//54	
0945+346	**//?//**	2,3	262 ± 7	0.67 ± .04	c-	CSS	<0.4	*	0945+346	EF			09 48 38.68	+34 23 17.6 16	
0949+354	**//?//**	2,3	336 ± 13	0.09 ± .07	+c-	C(2s)	11.3	*(VLBI)	0949+354	QSO 1.875	18.9	19.5	09 52 32.03	+35 12 52.4 16/40//85	+
0954+346	****//c**	2,3	322 ± 9	0.55 ± .09	c-	CSS	<0.3	*	0954+346	EF			09 57 46.34	+34 22 13.6 16	+
0955+320	**//?//c**	1	[728]	0.89 ± .02	s	II	128	1.4C	0955+320	GAL (0.18)	17.0	20.3	09 57 56.79	+31 50 41.5 17	+
0955+476	*c//?//c/*	1	619 ± 15	-0.33 ± .03	cpx	C+Di	20	(VLBI)	0955+476	XQSO 1.873	17.65	18.97	09 58 19.67	+47 25 07.8 25/43,45/52/67,85/X2	
0955+326	****//**	1	1520 ± 24	0.53 ± .04	cpx	C	0.3	*	0955+326	XQSO 0.533	15.55	15.91	09 58 20.96	+32 24 02.3 15.25//56,58/67,85/X2,X4	
0958+346	****//**	3	205 ± 5	(-0.3)	cpx	C	<1.2	*	0958+346	BSO			10 01 11.92	+34 24 50.4 Table A1	
1001+321	****//**	1	1230 ± 22	1.04 ± .03	c-	II	8.9	*	1001+321	GAL (0.90)	20.5		10 04 32.92	+31 51 51.5 14	
1003+351	**//?//**	1	4818 ± 97	0.71 ± .02	c-	II+cc	2340		1003+351	GAL 0.0989	15.02	17.18	10 06 01.73	+34 54 10.6 //51/70	
1003+498	**//?//**	2	335 ± 5	0.85 ± .01	c-	II	10.2	1.4A	1003+498	EF			10 06 32.35	+49 35 08.4 16	
1003+484	**//?//**	1,2	613 ± 20	1.16 ± .01	sb	II	9.5	*	1003+484	BSO	19.7	20.5	10 06 40.55	+48 13 09.4 14	+
1008+467	****//**	1	1505 ± 31	1.22 ± .03	c-	II	11.2		1008+467	GAL 1.781	22.5		10 11 45.28	+46 28 19.4 ///81	
1009+482	**//?//**	2	413 ± 16	0.98 ± .01	c-	II	4.6	1.4A	1009+482	EF			10 12 57.37	+47 58 03.8 16	
1010+495	**//?//**	2	283 ± 9	0.33 ± .03	cv?	C	<0.5	*	1010+495	BSO	19.29	<20.53	10 13 29.93	+49 18 41.0 16//53	
1010+346	****//**	2,3	284 ± 8	0.81 ± .03	c-	CSS	<0.5	*	1010+346	EF			10 13 36.21	+34 23 17.7 16	
1010+350	**//?//**	2,3	485 ± 14	-0.12 ± .06	+c-	C	0.4	*(VLBI)	1010+350	QSO 1.414	18.6	19.0	10 13 49.61	+34 45 50.8 16/40//67,85	
1011+496	**//?//**	2	472 ± 12	0.31 ± .05	-c+	C(2s)	0.4	1.4A	1011+496	XBL	15.49	16.56	10 15 04.14	+49 26 00.7 16//52//X2	
1012+488	**//?//**	2	532 ± 36	0.92 ± .01	c-	II+cc	110	1.4C	1012+488	QSO 0.385	18.9	19.5	10 15 57.63	+48 38 00.2 17//67,85	
1014+392	****//**	1	1391 ± 15	0.78 ± .01	c-	II?	7.7	1.4A	1014+392	GAL 0.206	17.7	20.0	010 17 13.84	+39 01 30.6 15///76	
1014+397	****//**	1	626 ± 26	1.05 ± .02	s	II	130	1.4P	1014+397	GAL (0.37)	19.5	21.0	10 17 18.32	+39 31 24.4 14	+

Table 3. continued

1015+491	***//**/*	1,2	589 ± 26	0.57 ± 0.2	c+	I	43	1.4A	1015+491	GAL (0.08)	14.82	16.90	o10 18 08.35	+48 53 33.2	15//52		
1015+359	/**//c**	1	653e(86)	(-0.2)	cpx	C(2s?)	4.4	*(VLBI)	1015+359	QSO 1.226	18.7	10 18 10.99	+35 42 39.4	25//44,45//67,85			
1016+329	****//**/*	1	631 ± 26	0.85 ± 0.3	c-	II	25	1.4A	1016+329	EF		10 19 19.14	+32 41 48.2	15			
1017+487	*tr//**/*	1,2	1849 ± 49	0.72 ± 0.2	s	II+cc	360	1.4C	1017+487	GAL 0.0520	15.09	10 20 53.66	+48 31 24.3	17//52/90		+	
1018+348	*/**//**/*	2,3	452 ± 10	0.17 ± 0.3	cpx	C(2s)	19	1.4A	1018+348	QSO 1.400	17.26	10 21 17.47	+34 37 21.6	16//52/67,85			
1020+481	*/**//**/*	2	479 ± 13	0.76 ± 0.1	s	CSS	0.5	*	1020+481	BSO	18.8	10 23 10.58	+47 51 46.8	16			
1020+486	*/**//**/*	2	253 ± 23	1.01 ± 0.3	s	II+cc	42	1.4A	1020+486	GAL	20.3	10 23 29.84	+48 24 37.2	16			
1024+463	****//**/*	1	1420 ± 98	0.92 ± 0.7	c-	II	71	1.4A	1024+463	GAL	20.3	o10 27 14.71	+46 02 48.0	15			
1024+485	****//**/*	1,2	993 ± 33	0.89 ± 0.2	c-	II+cc	78	1.4C	1024+485	GAL (0.28)	18.4	10 27 33.60	+48 17 18.5	17			
1025+389	****//**/*	1	786 ± 29	0.70 ± 0.4	c-	I?	?	*	1025+389	GAL 0.361	18.05	10 28 44.25	+38 44 36.7	15//50/60			
1031+504	***//**/*	1	1529 ± 12	0.99 ± 0.1	c-	II	3.1	*	1031+504	EF		10 34 17.85	+50 13 30.0	14			
1036+323	****//**/*	1	668 ± 16	0.96 ± 0.3	c-	II	7.3	1.4A	1036+323	EF		10 38 50.99	+32 06 05.8	15			
1037+497	*/**//**/*	2	323 ± 18	0.95 ± 0.4	c-	II	16	1.4A	1037+497	EF		10 40 17.94	+49 29 02.8	16			
1039+504	****//**/*	1	879 ± 31	1.23 ± 0.2	c-	II	66	*	1039+504	GAL (0.35)	18.7	o10 42 07.46	+50 13 21.0	14			
◊1042+392	****//c/*	1	663 ± 48	0.78 ± 0.2	s	II	11	*	1042+392	EF		10 45 15.06	+38 56 38.2	Table A1			
1044+476	**//**/*	1	806 ± 12	0.41 ± 0.2	+c-	C	0.6	*	1044+476	QSO 0.800	18.4	10 47 32.62	+47 25 31.9	15//67,85			
1045+352	****//**/*	1,2	1001 ± 12	0.73 ± 0.2	c-	CSS	<0.4	*	1045+352	EF		10 48 34.21	+34 57 24.8	15			
1048+347	*/**//**/*	2,3	510 ± 12	0.27 ± 0.4	cv	C	<0.5	*	1048+347	QSO 2.520	18.98	10 50 58.12	+34 30 10.9	16//591/67,85			
1049+344	****//**/*	1	759 ± 18	0.96 ± 0.2	c-	II	52	1.4A	1049+344	EF		10 51 58.23	+34 13 19.1	15			
1049+384	c//**/*	1	672 ± 20	0.77 ± 0.3	c-	CSS	<0.5	*	1049+384	QSO 1.018	20.6	10 52 11.76	+38 11 43.9	15//85		+	
1049+488	*/**//**/*	2	288 ± 23	0.92 ± 0.5	c-	II+cc	15	1.4A	1049+488	EF		10 52 17.55	+48 37 09.2	16			
1059+351	****//**/*	1,2	755 ± 14	0.86 ± 0.2	c-	I	12	1.4A,4.9A	1059+351	GAL (0.37)	18.8	11 02 08.66	+34 55 09.4	15,32			
1100+350	*/**//**/*	2,3	335 ± 12	1.03 ± 0.2	c-	II+cc	14	1.4A	1100+350	EF		11 03 26.25	+34 49 47.2	16			
1101+497	****//**/*	2	254 ± 7	0.55 ± 0.3	c-	CSS	<0.5	*	1101+497	BSO	19.1	11 04 26.90	+49 28 24.5	16			
1101+384	*/**//**/*	1	864 ± 17	(0.1)	cpx	C+Di	150	1.4C,(VLBI)	1101+384	XBL 0.0303	12.9	11 04 27.31	+38 12 31.8	5,15,17/43,45/58/68/X3			
1104+365	****//**/*	1	579 ± 15	0.91 ± 0.2	s	II+cc	24	1.4P,4.9A	1104+365	GAL 0.393	17.65	11 07 26.93	+36 16 12.2	14,32//50/60		+	
1105+392	****//c/*	1	890 ± 41	0.98 ± 0.5	s	II	69	1.4A	1105+392	QSO 0.781	18.6	11 08 36.32	+38 58 57.9	15//92			
1106+380	*c//**/*	1	1175 ± 21	0.43 ± 0.5	-c+	II?	1.3	*	1106+380	EF		11 09 28.86	+37 44 31.6	15			
1107+379	*c//**/*	1	2158 ± 27	0.85 ± 0.2	c-	II	78	1.4C	1107+379	GAL 0.346	18.7	o11 09 49.88	+37 38 31.0	17//77			
1107+349	//////?*	3	201 ± 6	-0.45 ± 0.31	cv	C	<0.4	*	1107+349	EF		11 10 04.82	+34 43 38.1	16			
1107+485	*/**//**/*	2	535 ± 10	0.44 ± 0.5	cv	C	<0.4	*	1107+485	XQSO 0.74	19.24	11 10 36.32	+48 17 52.5	16//591/X2			
1108+359	****//**/*	1	1229 ± 267	1.24 ± 0.3	cb	II	60	*	1108+359	GAL 1.105	21.5	o11 11 33.08	+35 40 41.8	17//79			
1113+349	****//**/*	2,3	403 ± 13	1.05 ± 0.3	c-	II	16	1.4A	1113+349	EF		11 16 30.47	+34 42 24.6	16			
1123+340	*c//**/*	1	1337 ± 150	0.90 ± 0.2	c-	CSS	<0.5	*	1123+340	EF		11 26 23.68	+33 45 26.9	15			
1124+498	*/**//**/*	2	523 ± 13	1.08 ± 0.3	c-	CSS	<0.3	*	1124+498	RO	20.3	11 27 09.69	+49 37 26.3	16			
1125+327	*c//**/*	1	606 ± 34	0.86 ± 0.2	c-	II+cc?	12	1.4A	1125+327	GAL (0.75)	20.0	11 28 02.48	+32 30 48.7	15			
1125+325	*c//**/*	1	697 ± 30	0.92 ± 0.3	c-	II	36	1.4A	1125+325	GAL (0.95)	22.	11 28 10.94	+32 15 51.6	15			
1127+507	*/**//c/*	1	[918]	0.95 ± 0.4	c-	CSS	0.6	*	1127+507	EF		11 29 47.93	+50 25 51.3	14			
◊1127+348	*/**//**/*	3	200 ± 17	0.99 ± 0.3	c-	II	35	*	1127+348	EF		11 30 05.9	+34 34 34.5	Table A1		+	
1128+385	*/**//c**	1	756e(87)	(-0.1)	cpx	C(1s)	<0.5	*(VLBI)	1128+385	QSO 1.733	19.24v	19.78	11 30 53.28	+38 15 18.6	15/41,43,45/53/85		

Table 3. continued

1129+351	**//**//**	2,3	366 ± 11	0.77 ± .06	c-	II	13	1.4A	1129+351	(GAL) 0.971	20.7	11 32 33.53	+34 53 20.6	16//60	+
1130+349	** _r **//**	1,2	561 ± 17	0.86 ± .03	c-	II	88	1.4P	1130+349	GAL 0.512	19.37	11 32 45.84	+34 39 36.7	14//50/71	
1130+339	***//**	1	933 ± 47	0.81 ± .03	c-	II+cc	28	1.4A	1130+339	GAL (0.19)	17.2	20.0	+33 43 12.3	15	
1130+504	**//**c**	1	854 ± 22	0.81 ± .02	cb	II+cc	10.1	1.4A	1130+504	GAL (0.31)	18.3	21.3	+50 08 40.1	15	
1130+335	***//**	1	760 ± 19	1.10 ± .03	c-	CSS	1.3	*	1130+335	BO	20.2	20.2	+33 18 06.3	14	
1131+493	**//**//c/*	1,2	1074 ± 417	0.89 ± .02	s	I+cc	>110	4.9P	1131+493	GAL 0.0335	13.52	15.41	+49 03 43.2	5,28//52/68	+
◇1131+492	**//**//c/*	2	[316]	0.69 ± .07	s?	I		*	1131+492	GAL (0.03)	14.5	16.6	+48 58 23.0	29	+
1132+374	**//**//**	1	634 ± 17	0.79 ± .02	c-	CSS	0.8	*	1132+374	EF			+37 08 40.9	15	
1135+480	**//**//**	2	319 ± 25	0.29 ± .07	c+	C(1s?)	11	1.4A	1135+480	EF			+47 45 15.4	16	
1136+505	**//**//c/*	1	618 ± 37	0.98 ± .01	c-	II	37	1.4P	1136+505	EF			+50 16 02.1	14	
1140+491	**//**//?/*	1,2	1015 ± 34	0.93 ± .02	c-	II	16	1.4A	1140+491	GAL (0.64)	19.6	21.5	+48 51 18.8	15	
1141+466	***//**c*	1	942 ± 38	1.01 ± .03	c-	II	9.5	4.9A	1141+466	GAL 0.162	15.77	17.97	+46 21 21.2	14,32//52/	
1141+354	***//**	2,3	284 ± 9	1.07 ± .03	c-	II	11	1.4A	1141+354	GAL 1.781	23.		+35 08 22.3	16//60	
1141+374	** _r **//**?	1	2190 ± 20	0.83 ± .03	c-	II	267	1.4P;B;BC	1141+374	GAL 0.1165	15.86	18.05	+37 08 41.7	6,8,14,30//52/63	
1143+500	**//**//**/*	1	1496 ± 40	1.19 ± .03	c-	II	4.3		1143+500	GAL 1.275	22.5		+49 46 07.5	///79	
1144+352	**//**//**	1	555v(99)	(-0.1)	cpx	C(2s)	27	1.4B,(VLBI)	1144+352	GAL 0.0630	14.66	16.74	+35 01 07.5	16,23/40,41/52/74	+
1144+497	*?//**//c/*	2	[251]	0.88 ± .03	s	II	34	1.4A	1144+497	BO	>20.3	19.9	+49 29 20.0	16	+
1145+485	**//**//**	2	498 ± 9	1.08 ± .02	c-	CSS	0.8	*	1145+485	EF			+48 18 49.5	16	
1148+366	***//**	1	568 ± 13	0.93 ± .02	c-	II	27	1.4P	1148+366	GAL 0.1412	18.40	20.4	+36 22 03.6	14//50/77	
1148+477	**//**//**/*	1	679 ± 30	1.08 ± .02	c-	II+cc	20	1.4A,4.9A	1148+477	QSO 0.867	16.84	17.5	+47 28 55.8	15,22//53/67,85	
1148+387	***//**	1	633 ± 16	0.93 ± .03	c-	I	9.2	1.4A	1148+387	QSO 1.299	16.60	17.22	+38 25 52.6	15//52/67,85	
1150+497	**//**//**	1,2	1860 ± 52	0.50 ± .04	s?	C(1s)	16.8	4.9A,(VLBI)	1150+497	XQSO 0.334	16.73	17.40	+49 31 08.8	22,26,27/43,45/52/67,85/X2	
1151+384	** _r **//c**	1	[1075]	0.80 ± .03	s	II+cc?	72	1.4P	1151+384	GAL 0.142	17.8	20.5	+38 11 47.7	15,31//69	+
1152+348	**//**//c**	3	218 ± 12	0.76 ± .03	c-	II	40	1.4A	1152+348	GAL (0.28)	18.2	21.5	+34 32 05.4	16	
1152+462	**//**//c/*	1	606 ± 44	0.28 ± .02	cv?	CSS?	1.6	*	1152+462	EF			+45 55 40.2	15	+
1155+486	**//**//**	2	330v(164)	(-0.1)	cpx	C	<0.1	*(VLBI)	1155+486	QSO 2.03	19.9		+48 25 16.2	40//66	
1157+460	***//**/*	1	1202 ± 19	0.87 ± .03	c-	CSS	0.8	*	1157+460	GAL 0.743	21.5		+45 48 42.5	14//94	
1158+351	** _r **//?/*	3	223 ± 13	1.03 ± .04	c-	II	139	1.4C	1158+351	GAL	20.5		+34 49 18.2	17	
1158+345	*c**//**	2,3	446 ± 19	0.80 ± .03	c-	II	38	1.4A	1158+345	GAL	20.5		+34 16 55.4	16	+
1159+395	**//**//**/*	1	613 ± 14	0.54 ± .03	cv	CSS	0.8	*	1159+395	EF			+39 19 11.4	15	
1202+492	**//**//?/*	2	252 ± 18	0.79 ± .02	c+	II+cc	12	1.4A,4.9A	1202+492	QSO 0.446	17.31	18.30	+48 56 54.0	16,32//52/72,85	
1202+350	**//**//**	3	226 ± 9	0.76 ± .04	c-	II+cc	30	1.4A	1202+350	EF			+34 46 13.4	16	
1202+499B	c//**//c/c	2	[317]	0.74 ± .01	s	II+Di	18	1.4C,4.9B	1202+499B	GAL (0.30)	18.4	21.3	+49 40 23.8	17,20	+
1202+485	**//**//c/*	2	534 ± 18	0.89 ± .02	c-	CSS	2.6	*	1202+485	EF			+48 17 54.2	16	
1203+499	**//**//c/*	2	[269]	0.81 ± .06	c-	CSS	1.0	*	1203+499	EF			+49 40 44.1	17,20	
1204+371	***//**	1	612 ± 18	1.08 ± .04	c-	II	51	1.4P	1204+371	EF			+36 51 40.3	14	
1204+353	***//**	2,3	505 ± 15	1.12 ± .03	c-	II+cc	18	1.4A	1204+353	RO	22.		+35 03 06.5	16	
1205+392	** _r **//**	1	658 ± 24	0.94 ± .02	c-	I+cc	28	1.4P	1205+392	GAL 0.2435	17.8	20.7	+38 56 00.8	14//77	
1211+486	**//**//**/*	2	455 ± 43	1.06 ± .05	c-	II+cc	61	1.4A	1211+486	EF			+48 23 13.9	16	
1211+334	**//**//**	1	1289 ± 22	0.37 ± .02	cv?	CSS	<0.4	*	1211+334	XQSO 1.598	17.10	17.84	+33 09 45.6	15//52/67,85/X2	

Table 3. continued

1213+350	****//**	1,2	1522v(163)	0.34 ± 0.2	cv?	C(2s)	14	*(VLBI)	3+350	QSO 0.857	20.5	20.0	12 15 55.60	+34 48 15.2	25/43,45//67,85	
1216+507	**r//**/*	1	596 ± 26	0.84 ± 0.3	c-	II	196	1.4C	6+507	GAL (0.25)	17.8	19.7	o12 18 49.91	+50 26 16.7	17	
1216+475	*//**/*	1	826 ± 34	0.76 ± 0.1	c-	I+cc	420	1.4BC _i C	6+475	GAL 0.0022	9.2		12 18 57.52	+47 18 14.3	5,11,30//68	+
1216+487	*//**/*	1,2	899 ± 18	(-0.0)	cpX	C(1s)	10	*(VLBI)	6+487	QSO 1.076		18.7	12 19 06.42	+48 29 56.2	25/43,45//67,85	
1217+348	*//**/*	3	220 ± 7	(0.0)	cpX	C	<0.4	*	7+348	BL	16.52	17.71	12 20 08.29	+34 31 21.7	16//52	
1218+339	****/*?*	1	2632 ± 35	0.97 ± 0.4	-c+	II+cc	9.4	4.9A,15A	8+339	XQSO 1.519	18.80	18.80	12 20 33.89	+33 43 09.9	13//57/67,85/X4	
1218+489	*//**/*	2	318 ± 23	0.92 ± 0.3	c-	II?	2.8	1.4A	8+489	BO	20.7	20.7	12 21 10.81	+48 42 39.7	16	+
1221+484	*//**/*	2	347 ± 9	0.46 ± 0.3	cv	CSS	<0.3	*	1+484	BZO	20.4	21.1	12 23 58.18	+48 12 57.7	16	
1223+395	****//**	1	579 ± 16	0.12 ± 0.2	cv	C(2s)	12.5	1.4A _v (VLBI)	3+395	QSO 0.623	20.60		12 25 50.57	+39 14 22.7	15/40/54/66	
1225+368	*//**/*	1	2151 ± 40	0.20 ± 0.4	cv	CSS	<0.1	*(VLBI)	5+368	QSO 1.973	21.3		12 27 58.73	+36 35 11.8	45//85	
1226+492	*//**/*	2	399 ± 14	0.57 ± 0.8	+c-	C	<0.3	*	6+492	NSO	18.58	19.82	12 28 51.77	+48 58 01.3	16//591	+
1230+486	ccc//c/c	2	377 ± 40	(0.0)	cpX	C	<0.3	*	0+486	BZO	21.03	21.5	12 32 34.80	+48 21 33.0	16//54	+
1230+349	****//**	2,3	478 ± 11	1.07 ± 0.3	c-	II	11	1.4A	0+349	GAL 1.533	22.2		12 32 41.38	+34 42 50.6	16//60	
1231+481	*//**/*	2	374 ± 18	0.04 ± 0.6	cv	CSS	<0.5	*	1+481	XQSO 0.375	16.51	17.53	12 34 13.33	+47 53 51.2	16//52/72,85/X2	
1231+495	****//**	2	329 ± 17	1.11 ± 0.1	c-	II	29	1.4A	1+495	EF?			12 34 20.89	+49 14 27.7	16	+
1234+371	****//**	1	880 ± 18	1.01 ± 0.4	c-	II	19	1.4A	4+371	EF			12 36 50.00	+36 55 18.3	15	
1236+327	****//**	1	785 ± 16	0.85 ± 0.1	c-	II	3.8	*	6+327	EF			12 39 09.10	+32 30 27.5	15	
1237+353	*c//c**	3	227 ± 15	1.04 ± 0.6	c-	II+cc	18	1.4A	7+353	QSO 1.194	16.81	17.50	12 40 21.13	+35 02 58.8	16//52/72,85	+
1239+328	r//**/*	1	1187 ± 52	0.91 ± 0.4	-c+	Disk	660	1.4C,D	9+328	GAL 0.0022	10.0		12 42 06.86	+32 32 34.1	4,5,10,17//68	+
1239+376	*//**/*	1	569 ± 12	(0.0)	cpX	C	<0.1	*(VLBI)	9+376	QSO 3.818	19.5		12 42 09.81	+37 20 05.7	40//92	
1242+364	****//**	1	776 ± 14	0.99 ± 0.1	c-	CSS	1.5	*	2+364	BO	19.8	20.4	12 44 49.70	+36 09 25.4	14	
1244+389	****//**	1	620 ± 23	1.14 ± 0.3	c-	II	24	1.4P	4+389	EF			12 46 46.15	+38 41 39.4	14	
1244+492	*c//**/*	1,2	1176 ± 19	0.56 ± 0.1	(s)	II	3.2	*	4+492	GAL 0.207	17.4	20.3	12 47 07.37	+49 00 18.2	15//87	
1247+336	**//**/*	1	1435 ± 37	0.81 ± 0.2	c-	II	78	*	7+336	GAL (0.35)	18.8	21.4	o12 49 51.13	+33 23 19.5	17	
1248+350	c//**/*	2,3	266 ± 9	0.83 ± 0.2	c-	II?	2.6	*	8+350	QSO 0.972	19.9	20.2	12 50 33.37	+34 43 56.7	16//67	+
1249+508	****//**	1	1304 ± 68	1.06 ± 0.3	sb	II	138	*	9+508	GAL 0.414	20.0		12 51 43.59	+50 34 25.1	17//84	+
1249+475	****//**	1	981 ± 23	1.10 ± 0.3	c-	II	45	1.4P	9+475	EF			12 52 16.70	+47 15 38.4	14	
1251+348	*//**/*	2,3	359 ± 16	0.73 ± 0.3	s	II	38	1.4A	1+348	GAL	19.8		12 53 24.32	+34 35 10.5	16	
1253+353	*//**/*	2,3	286 ± 5	0.88 ± 0.3	s	II	2.9	*	3+353	EF?			12 56 11.31	+35 02 18.7	16	
1253+375	****//**	1	700 ± 8	1.07 ± 0.2	c-	II	40	1.4P	3+375	EF			12 56 17.62	+37 13 43.5	14	
1254+476	****//**	1	5246 ± 84	0.86 ± 0.1	c-	II	12.9	*	4+476	XGAL 0.994	21.0		12 56 57.56	+47 20 20.2	///70/X1	
1255+370	****//**	1	742 ± 13	0.84 ± 0.3	c-	CSS	0.9	*	5+370	QSO 0.283	18.2	17.8	12 57 23.86	+36 44 19.9	15//67,85	
1256+489	****//c/	2	[314]	1.03 ± 0.3	s	II	40	*	6+489	EF			12 59 11.44	+48 41 31.6	17	+
1257+383	****//**	1	755 ± 23	1.03 ± 0.3	c-	II	35	1.4A	7+383	EF			13 00 13.57	+38 04 30.3	15	
1258+353	*//**/*	3	220 ± 5	0.93 ± 0.5	c-	II	41	*	8+353	EF			13 00 48.04	+35 05 28.8	17	
1301+382	****//**	1	597 ± 26	0.92 ± 0.2	c-	II	31	1.4A	1+382	GAL 0.470	18.61	20.8	13 03 43.96	+37 56 09.3	15//50/71	
1301+354	*//**/*	2,3	471 ± 14	0.66 ± 0.3	c-	CSS	0.9	*	1+354	EF			13 03 53.76	+35 09 50.8	17	
1308+326	****//**	1	1405v(284)	(0.0)	cpX	C(1s)	11	1.4A _v (VLBI)	8+326	XBL 0.996	15.61v		13 10 28.66	+32 20 43.8	15/41,47/58/67,85/X2	
1309+327	****//**	1	645 ± 25	1.08 ± 0.4	c-	II	9.1	1.4P	9+327	EF			13 11 49.50	+32 27 48.9	14	
1310+487	*//**/*	2	255 ± 17	(0.0)	cpX	C+Di	4.0	1.4A	0+487	RO	20.11	>21.8	13 12 43.35	+48 28 30.9	16//54,591	

Table 3. continued

1315+396	****//**	1	622 ± 14	0.57 ± .13	-c+	C(2s)	2.8	1.4A	1315+396	QSO	1.560	18.12	19.0	13 17 18.64	+39 25 28.7	14.19//53.58/85	
1315+346	*//**//***	1,2	604 ± 14	0.27 ± .10	+c-	C(1s)	1.7	*	1315+346	QSO	1.050		18.5	13 17 36.49	+34 25 15.9	25//67.85	
1318+345	*//**//***	2,3	493 ± 17	0.86 ± .02	c-	II+cc?	16	1.4A	1318+345	BO			20.5	13 21 05.51	+34 15 01.0	16	
1320+325	****//***	1	826 ± 24	0.97 ± .01	c-	II+cc	5.3	1.4P,4.9A	1320+325	EF				13 22 47.11	+32 16 11.0	14.32	
1322+366	****//***	1	917 ± 23	0.58 ± .02	c-	I+cc	45	1.4A,B	1322+366	GAL	0.0175	12.92	14.80	013 24 51.46	+36 22 43.4	3.5,7,17,23//52/77	+
1323+370	****//***	1	1024 ± 50	0.70 ± .02	(s)	II	29	1.4A	1323+370	GAL	(0.08)	15.00	17.04	13 26 02.37	+36 47 59.4	15//52	
1324+498A	**r//**c/c	1	641 ± 48	0.90 ± .03	s	II	165	1.4C	1324+498A	EF				13 26 14.26	+49 34 35.9	17	+
1323+321	?c**//***	1	4681 ± 54	0.48 ± .01	c-	CSS	<0.1	*(VLBI)	1323+321	GAL	0.369			13 26 16.51	+31 54 09.5	25//47//93	
1324+348	*//**//c**	3	206 ± 8	0.75 ± .09	-c+	C	<0.4	*	1324+348	EF				13 27 16.03	+34 32 35.3	16	
1325+321	*//**//**/*	1	1454 ± 44	0.66 ± .03	c-	I+cc	26	1.4A,4.9A	1325+321	GAL	(0.26)	18.0	20.4	13 27 31.66	+31 51 27.5	15.32	
1327+474	**//**//**/*	1	1380 ± 66	0.86 ± .16	sb	Disk	350	1.4C	1327+474	GAL	0.0018	8.9		13 29 51.80	+47 11 45.5	4.5,9,14,30//68	+
1329+503	*c*//**c/*	1	1093 ± 43	0.97 ± .05	c-	II	41	1.4P	1329+503	EF				13 31 37.33	+50 07 53.5	14	+
1335+479	****//**/*	1	794 ± 17	0.73 ± .01	c-	II	8.5	1.4A	1335+479	GAL	(0.42)	19.3	21.5	013 37 38.66	+47 41 46.2	15	
1336+390	****//***	1	3560 ± 59	0.99 ± .01	c-	I+cc	>26		1336+390	GAL	0.246	17.7		13 38 49.90	+38 51 10.0	///70	
1339+472	***//**//**/*	1	677 ± 12	0.96 ± .01	c-	II	24	1.4A	1339+472	GAL	(0.40)	19.2	20.7	013 41 44.97	+46 57 18.4	15	
1340+353	****//***	1,2	844 ± 23	0.79 ± .01	s	II+cc	20	1.4A	1340+353	BO			21.3	13 42 31.80	+35 07 10.3	15	
1340+319	****//**/*	1	693 ± 18	0.89 ± .04	c-	II	23	1.4A	1340+319	EF				13 43 03.00	+31 43 48.6	15	
1343+500	***//**//**/*	1	2398 ± 36	0.99 ± .01	c-	II+cc	10.1		1343+500	XGAL	0.967	22.6		13 45 26.24	+49 46 32.5	///80/X1	
1343+386	?****//***	1	893 ± 25	0.59 ± .01	s	II?	14	1.4A	1343+386	QSO	1.844	18.2	18.7	013 45 36.98	+38 23 12.4	15//67.85	
1344+484	****//**//**/*	1	589 ± 18	0.83 ± .02	c-	II	3.1	*	1344+484	EF				13 46 23.82	+48 13 05.6	15	
1348+352	****//**//**/*	2,3	509 ± 12	0.80 ± .02	c-	I?	31	1.4A,4.9A	1348+352	EF				13 51 01.18	+34 59 44.2	16,32	+
1354+325	****//**//**/*	1	644 ± 16	1.08 ± .02	c-	II	74	1.4P	1354+325	GAL	(0.35)	18.8	20.5	013 56 44.94	+32 19 51.8	14	+
1356+478	////**//**/*	1	614 ± 14	-0.20 ± .10	cv	CSS	<0.3	*	1356+478	GAL	0.230	18.1	21.0	13 58 40.66	+47 37 58.5	15//92	
1400+347	*//**//**//**/*	2,3	262 ± 5	0.78 ± .02	s	C+Di	5.4	1.4A	1400+347	EF				14 02 35.75	+34 28 20.7	16	
1401+387	**//**//**//**/*	1	699 ± 27	0.85 ± .02	c-	II	71	1.4A	1401+387	EF				14 03 11.80	+38 27 56.1	15	
1401+353	****//**//**/*	1,2	654 ± 21	0.94 ± .02	c-	II	4.8	1.4A	1401+353	GAL	(0.45)	19.5	21.4	14 03 19.31	+35 08 12.8	15	
1404+344	****//**//**/*	1	1333 ± 25	1.23 ± .02	c-	II	15.8	1.4A	1404+344	XGAL	1.786			14 06 44.10	+34 11 25.9	15//84/X1	
1404+347	////**//**/*	3	197 ± 7	(0.0)	cpX	C	<0.4	*	1404+347	XQSO		18.2	18.8	14 06 53.84	+34 33 37.3	16//X2	
1405+517	**r//**//**/*	1	658 ± 30	0.98 ± .03	c-	II	140	1.4P	1405+517	GAL	(0.40)	19.2	21.3	014 07 18.35	+51 32 03.1	14	
1408+370	****//**//**/*	1	1224 ± 22	0.79 ± .01	c-	CSS	<0.5	*	1408+370	EF				14 10 42.97	+36 47 21.3	15	
1412+352	*//**//**//**/*	2,3	408 ± 11	0.94 ± .02	c-	II	20	1.4A	1412+352	BO			21.5	14 14 25.22	+34 58 44.9	16	
1413+349	///?//**//**/*	1	2054 ± 31	0.42 ± .07	cv	CSS	<0.5	*	1413+349	EF				14 16 04.18	+34 44 36.4	25	+
1414+482	****//**//**/*	1	748 ± 29	1.11 ± .03	c-	II+cc	42	1.4P	1414+482	EF				14 16 44.63	+48 02 51.5	14	
1415+463	****//**c/*	1	902 ± 17	0.50 ± .01	cpX	C(1s)	11.8	4.9A,(VLBI)	1415+463	QSO	1.552	17.5	18.4	14 17 08.16	+46 07 05.5	22,25,26,27/40//67,85	+
1420+326	*//**//**//**/*	1	566 ± 31	(0.1)	cpX	C	<1.3	*	1420+326	QSO	0.685	17.6	17.2	14 22 30.38	+32 23 10.4	Table A1//67,85	
1423+352	*//r//**//**/*	3	210 ± 8	0.80 ± .01	s	I	73	1.4C	1423+352	GAL	(0.37)	19.0	21.1	14 25 41.41	+34 58 28.6	17	
1426+346	*//**//**//**/*	2,3	256 ± 6	1.00 ± .01	c-	CSS	0.6	*	1426+346	EF				14 29 05.12	+34 26 41.0	16	
1436+340	*c*//**//**/*	1	576 ± 19	0.93 ± .02	s	II	8.5	1.4A	1436+340	EF				14 38 48.95	+33 50 14.7	15	
1438+385	*//**//**//**/*	1	1033 ± 12	(0.2)	cpX	C(1s?)	8.9	1.4A,(VLBI)	1438+385	QSO	1.775	21.6		14 40 22.34	+38 20 13.6	15,45//43,45//92	
1442+507	****//**//**/*	1	1224 ± 19	0.78 ± .02	c-	CSS	0.5	*	1442+507	EF				14 43 43.26	+50 34 30.8	15	

